Annales Societatis Geologorum Poloniae (2026), vol. 96: 157–174 https://doi.org/10.14241/asgp.2026.07

This is an open access article under the CC BY license
(http://creativecommons.org/licenses/by/4.0/),
which permits use, distribution, and reproduction
in any medium, provided that the article is properly cited.

SEDIMENTARY RECORD OF RIVER FLOODS IN THE MIDDLE MIOCENE LIGNITES OF THE KONIN BASIN (CENTRAL POLAND): SHORT- VERSUS LONG-DURATION FLOODS

Lilianna CHOMIAK[1], **Jakub KLĘSK**[2], **Paweł URBAŃSKI**[3], **Robert WACHOCKI**[4], **Marek WIDERA**[2]*

[1] *District Authority Office in Poznań, Jackowskiego 18, 60-509 Poznań, Poland; e-mail: chomiak@amu.edu.pl,*
[2] *Institute of Geology, Adam Mickiewicz University, Krygowskiego 12, 61-680 Poznań, Poland; e-mails: jakub.klesk@amu.edu.pl, widera@amu.edu.pl,*
[3] *Polish Geological Institute – National Research Institute, Rakowiecka 4, 00-975 Warszawa, Poland; e-mail: purb@pgi.gov.pl,*
[4] *Konin Lignite Mine, 600-lecia 9, 62-540 Kleczew, Poland; e-mail: robert.wachocki@vp.pl,*
* *Corresponding author*

Chomiak, L., Klęsk, J., Urbański, P., Wachocki, R. & Widera, M., 2026. Sedimentary record of river floods in the Middle Miocene lignites of the Konin Basin (Central Poland): Short- versus long-duration floods. *Annales Societatis Geologorum Poloniae*, 96: 157–174.

Abstract: Two stratigraphically distinct main lignite seams have been mined in the Konin Basin (central Poland) for decades. These seams originated during two peaks of the Middle Miocene Climatic Optimum, when widespread mires developed as backswamps in the vicinity of river channels. Weather fluctuations likely caused frequent flooding, recorded within the lignite seams as siliciclastic lithosomes or high concentrations of mineral matter in specific lignite layers (e.g., high ash yields). Facies analysis of selected sandy lithosomes in the opencast lignite mines near the town of Konin (Lubstów, Jóźwin IIB, and Tomisławice) illustrates a wide range of sedimentary facies and deformational structures. While some of these facies formed subaerially, others were deposited under subaqueous conditions in shallow, ephemeral lakes on the surface of Middle Miocene mires. Nonetheless, all the studied sediments are typical of crevasse splays or small lacustrine deltas, deposited near inferred meandering and/or anastomosing river channels. Consequently, the subaerial facies are attributed to high-energy, relatively short floods, whereas the subaqueous ones are linked to low-energy, slowly evolving regular floods. This hypothesis relies on the relationship between the rate of rising water levels in the river channel and the adjacent mire area, which is primarily controlled by the permeability of natural levee sediments.

Key words: Neogene, facies analysis, overbank siliciclastic sediments, lignite seams, crevasse splays, flood-basin swamps.

Manuscript received 22 March 2026, accepted 31 August 2026

INTRODUCTION

The mineral matter present in coal of various ranks, including lignite, is an integral part of explored and mined seams. It occurs in the form of layers, lenses, veins, and clastic dykes, and is also dispersed within the organic matter. In the former case, the siliciclastic sediments are macroscopically visible in borehole cores as well as in underground and opencast exposures. Within the organic matter, the clastic content can be determined as ash yield by combusting coal samples. The presence of mineral matter within a coal seam reduces its quality – primarily the net calorific value – and affects other geological and mining parameters, such as the stripping ratio (e.g., Markič and Sachsenhofer, 2010; Flores and Moore, 2024). High concentrations of siliciclastic material render the coal unsuitable for certain applications

(e.g., in energy or chemical industries) or require selective mining (e.g., Vessey and Bustin, 2000; Thomas, 2013; Michaelsen and Demberelsuren, 2024; Kędzior *et al.*, 2025).

Studies of non-coal interlayers and the surrounding strata, including siliciclastic sediments, within global lignite deposits are relatively common. Their identification relies primarily on borehole and geophysical data (Markič and Sachsenhofer, 1997; Holdgate *et al.*, 2002; Schäfer and Utescher, 2014; Michaelsen and Demberelsuren, 2024, and references therein), as well as surface outcrops (Rajchl *et al.*, 2008; Mach *et al.*, 2013; Prinz *et al.*, 2017, and references therein). One notable exception is the Velenje Lignite Mine in Slovenia, where such research was also conducted underground (Markič and Sachsenhofer, 2010).

The presence of siliciclastic sediments (mud, sand, and gravel) within the lignite-dominated succession of the study area has long been recognised, through both exploration-stage research and subsequent mining (e.g., Widera, 2016; Chomiak *et al.*, 2019; Dziamara *et al.*, 2023; Widera *et al.*, 2024). In the opencast lignite mines of the Konin Basin, the use of relatively shallow boreholes (ranging from several tens of metres to around 280 m in depth) historically allowed mining companies to avoid uneconomic, clastic-rich lignite seams. However, as extraction expanded, encountering these sand-rich interbeds became inevitable. Conversely, from a scientific perspective, their exposure has provided excellent opportunities for sedimentological studies (e.g., Widera *et al.*, 2023, 2024, 2026; Kasztelewicz *et al.*, 2025).

Lignite in the Konin Basin has been extracted from 12 opencast mines, primarily for electricity generation. For decades, mining targeted the axial, thickest parts of the deposits where clastic interbeds were exceptionally rare. However, as these central reserves neared depletion, operations expanded into seam margins, containing frequent siliciclastic interbeds (Naworyta and Urbański, 2025). Early sedimentological observations of these interbeds, such as the sandy lithosome in the Lubstów opencast mine (Fig. 1), were conducted prior to 2015 but remained unpublished. A key turning point occurred in 2015 with the discovery of a major sandy body in the Tomisławice opencast mine (Widera, 2016, 2017). Subsequent investigations in the Jóźwin IIB and Tomisławice mines revealed further substantial sandy and clayey interbeds (Fig. 1; Chomiak *et al.*, 2019; Dziamara et al., 2023; Widera *et al.*, 2024), which have been interpreted as subaerial and subaqueous crevasse splays (Widera *et al.*, 2023).

The main aim of this study is to analyse the facies of selected fine-grained sandy lithosomes, occurring within the lignite seams exploited in the Konin Basin. This is achieved through three secondary objectives: 1) the description and interpretation of sedimentary and deformational facies, 2) the distinction between subaerial and subaqueous facies, and 3) the formulation of two conceptual models for the formation of crevasse splays and microdeltas during short- and long-duration regular floods. Consequently, this study tests the hypothesis that differences in sedimentary facies reflect varying flood dynamics.

GEOLOGICAL SETTING

The examined sediments were exposed in the Lubstów, Jóźwin IIB, and Tomisławice opencast lignite mines, near Konin (Konin Basin) in central Poland (Fig. 1). All three mines are located within fault-bounded tectonic grabens, with depths ranging from several tens of metres (Jóźwin IIB and Tomisławice) to over 240 m (Lubstów). Their Mesozoic basement comprises Upper Cretaceous rocks, primarily

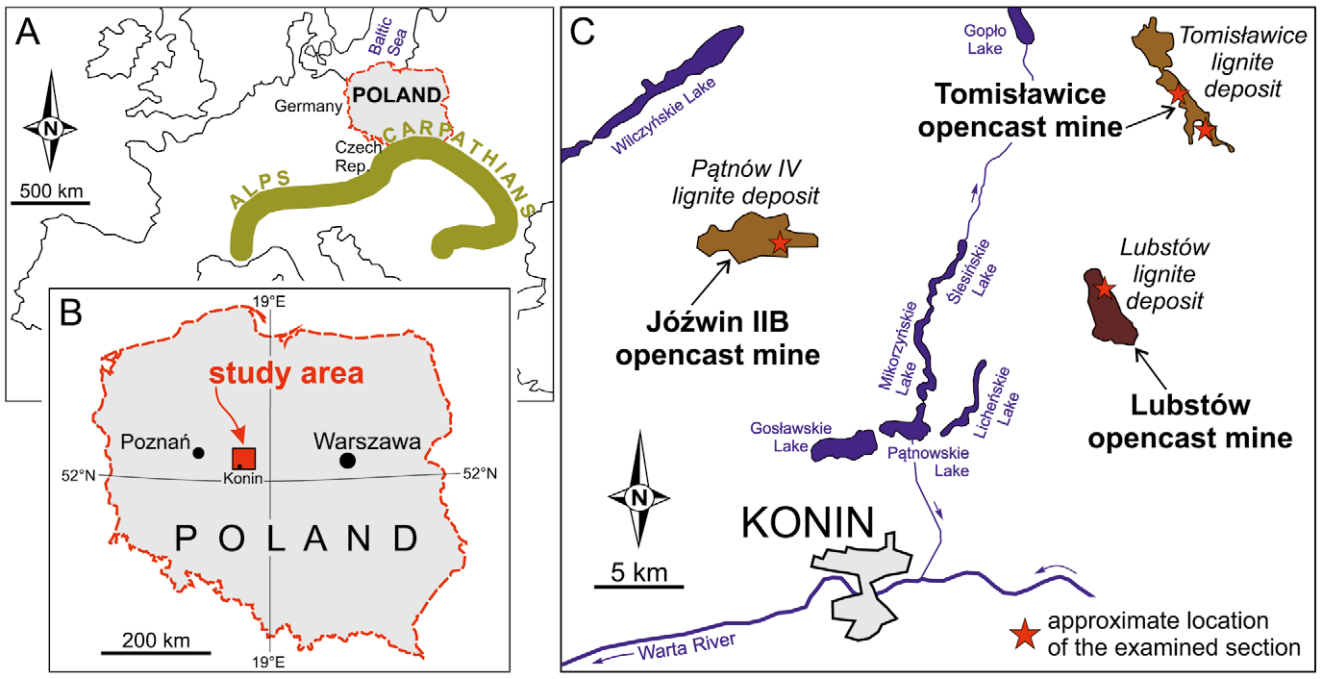


Fig. 1. Location maps. **A.** Poland on a map of Europe. **B.** Study area on a map of Poland. **C.** Location of the examined sections within lignite opencast mines in the Konin Basin. Geographical coordinates of the sections: Lubstów – 52°22′54.8″N, 18°27′46.4″E; Jóźwin IIB – 52°24′13.2″N, 18°10′56.7″E; Tomisławice South – 52°27′06.3″N, 18°31′46.3″E; Tomisławice North – 52°28′20.7″N, 18°30′38.7″E.

marls and carbonate sandstones (Ciuk and Grabowska, 1991; Widera, 2021, 2024). The Cenozoic succession – which differs in lithology and lithostratigraphic completeness across the studied areas – forms a continuous unit, ranging from 50 to over 280 m in thickness.

Due to a significant hiatus spanning the Paleocene to early Oligocene – characterised by non-deposition and subsequent erosion, caused by tectonic uplift in central Poland – the Paleogene in the Lubstów and Tomisławice areas is represented exclusively by lower Oligocene (Rupelian) sediments (Figs 2, 3, 4B). These deposits consist mainly of marine glauconitic sands and muds, ranging in thickness from up to 10–15 m in Tomisławice to over 130 m in Lubstów. Conversely, no Paleogene sediments have been identified in the area of the Jóźwin IIB opencast mine, either in borehole data or mine exposures (Figs 2, 4A).

The Neogene in the study area begins with terrestrial sediments deposited following the late Oligocene (Chattian) tectonic uplift of the Polish Lowlands. Initially, subcoal sands and carbonaceous (coaly) sands with lignite lenses (Rawicz Formation) accumulated in the Lubstów area. Peat accumulation took place in this region during the latest phase of the Early Miocene and the early Middle Miocene. This peat was subsequently transformed into the lignite of the present 2nd Lusatian Lignite Seam (LLS-2), which reaches a maximum thickness of 86.2 m at Lubstów. Lithostratigraphically, the LLS-2 belongs to the Ścinawa Formation (Fig. 2; Piwocki and Ziembińska-Tworzydło, 1997; Widera, 2024). Based on palynological data (Ciuk and Grabowska, 1991), the LLS-2 accumulated during the first peak of the Middle Miocene Climatic Optimum (Zachos *et al.*, 2001; Bruch *et al.*, 2007), under a warm, temperate to subtropical climate (Kasiński and Słodkowska, 2016).

In the area of the Jóźwin IIB and Tomisławice opencast mines, the subcoal sands and carbonaceous sands are similar to those in the Lubstów mine and are classified as the Koźmin Formation (Fig. 2). Peat accumulated there between 15.1 and 14.3 Ma, corresponding to the middle part of the Middle Miocene (Widera *et al.*, 2021a, b). It currently forms the 1st Mid-Polish Lignite Seam (MPLS-1), which has an average thickness of 6.8 m but locally exceeds 13.0 m (Figs 3, 4; Wachocki *et al.*, 2020; Widera, 2021). The MPLS-1 belongs to the lower part (Grey Clay Member) of the Neogene Poznań Formation (Fig. 2; Piwocki and Ziembińska-Tworzydło, 1997; Widera and Klęsk, 2025). The MPLS-1 accumulated during the final peak of the Middle Miocene Climatic Optimum (Zachos *et al.*, 2001; Bruch *et al.*, 2007; Kasiński and Słodkowska, 2016), under a warm-temperate and humid climate (Słodkowska and Widera, 2021, 2022).

The LLS-2 and MPLS-1 are overlain by Neogene fluvial and Quaternary glaciogenic sediments, ranging in thickness from 40 to over 80 m (Figs 3, 4). The Neogene sequence terminates with multicoloured muds (i.e., 'green clays' and 'flaming clays'), which constitute the upper part of the Poznań Formation, specifically the Wielkopolska Member (Fig. 2; Piwocki and Ziembińska-Tworzydło, 1997; Widera and Klęsk, 2025). These muds represent sediments of a late Neogene anastomosing (e.g., Widera *et al.*, 2021b; Urbański *et al.*, 2025) or anastomosing-to-meandering transitional fluvial system (Zieliński and Widera, 2020; Kędzior *et al.*, 2021). They are in turn overlain by glaciogenic Pleistocene sediments (tills, gravels, sands, and muds), a thin cover of Holocene alluvial sediments (<1.5 m thick), and modern soil.

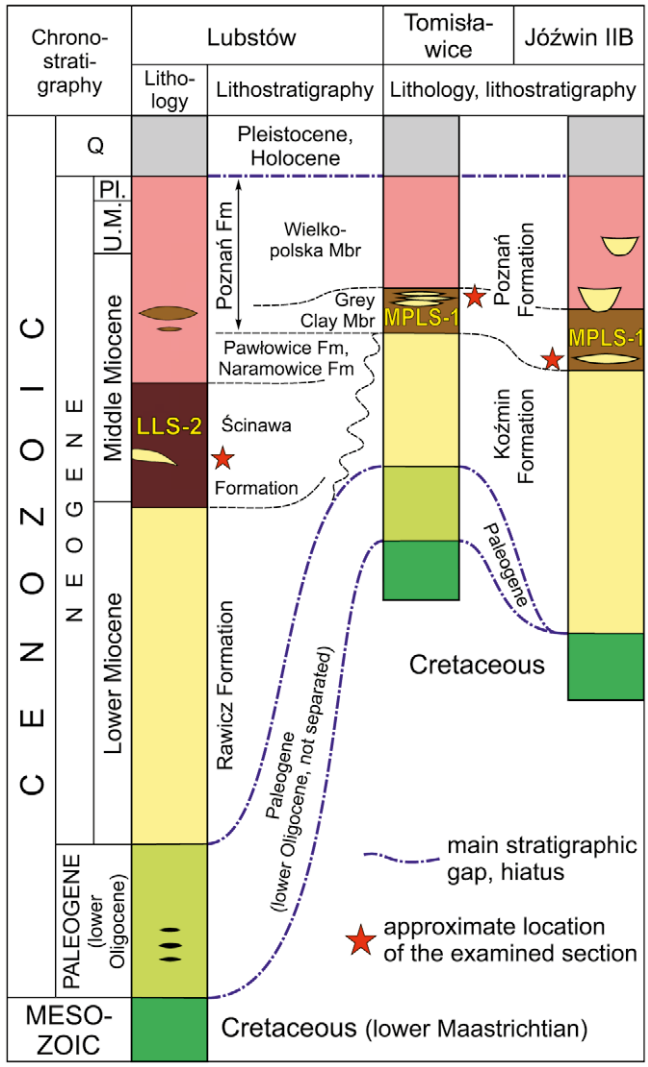


Fig. 2. Generalised lithostratigraphy of areas with mined lignite seams in the Konin Basin. Note the approximate stratigraphic position of the examined siliciclastic sediments within the lignite seams; for explanations, see Figure 3.

MATERIALS AND METHODS

The examined sandy lithosomes were positioned between lignite benches of exploited lignite seams, i.e., LLS-2 at Lubstów and MPLS-1 at Jóźwin IIB and Tomisławice (Fig. 2). In both cases, the lithosomes were easily accessible for direct field observations over distances exceeding 0.5–1.0 km in various directions. The maximum thickness of the siliciclastic interbeds exposed within LLS-2 and MPLS-1 is around 4.8 m. In this study, four vertical sections of these interlignite sediments were selected for detailed facies analysis. Fieldwork was carried out from 1995 to 2004 in the Lubstów opencast mine, and between 2015 and 2025 in the Jóźwin IIB and Tomisławice mines.

On the basis of data from several dozen boreholes, three representative geological cross-sections through the Cenozoic succession of the study areas were constructed (Figs 3, 4). Boreholes at Jóźwin IIB and Tomisławice generally reached depths of less than 100 m, whereas those at Lubstów mostly exceeded 100 m, reaching a maximum depth of >280 m. These borehole data, along with other cartographic materials (e.g., mining maps), were obtained from the geological archive of the Konin Lignite Mine at Kleczew, near Konin.

All interlignite siliciclastic sediments were documented photographically in the field (Figs 5–12). For all cross-stratified sands (planar or trough), multiple palaeoflow measurements were taken. Hundreds of siliciclastic samples were analysed for their granulometry, ash yield, and ash composition (e.g., Widera, 2016; Dziamara *et al.*, 2023; Widera *et al.*, 2026), enabling a precise definition of the sediment type. Consequently, for grain-size classes and subclasses, the standard classification scheme of Wentworth (1922) was applied. For sand–silt–clay mixtures, the scheme of Folk (1974) was used. For example, the term 'muddy sand' corresponds to a sediment composed of over 50 wt% sand and under 50 wt% silt and clay combined. Where fine-grained sediments contain gravel-sized (>2 mm) intraclasts (rip-up clasts), the term 'gravel' or 'gravelly' was appended to the sediment name.

The examined siliciclastic sediments were classified and interpreted using facies analysis of fluvial deposits, following Miall (2006, 2022), Boggs (2012), and Zieliński (2014). To simplify the description of facies identified in the field, the coding system originally proposed by Miall (1977) for clastic rocks was applied (Tab. 1). Most letter codes for sedimentary textures and structures follow Miall (1977), except for the code 'M', introduced for mud by Widera *et al.* (2019). Facies coding follows a straightforward convention: textural attributes are denoted by capital letters, whereas

Table 1

Textural and structural codes, used in this study to describe sediment facies (after Miall, 1977, supplemented). For descriptions and interpretations of the facies associations see Table 2 and the text.

Facies code	Facies texture
G	gravel
S	sand
M	mud
C	coal, carbonaceous
	Facies structure
m	massive
h	horizontal (plane-parallel) lamination
p	planar cross-stratification
t	trough cross-stratification
r	ripple cross-lamination
d	deformed (folded, faulted, fractured, etc.)

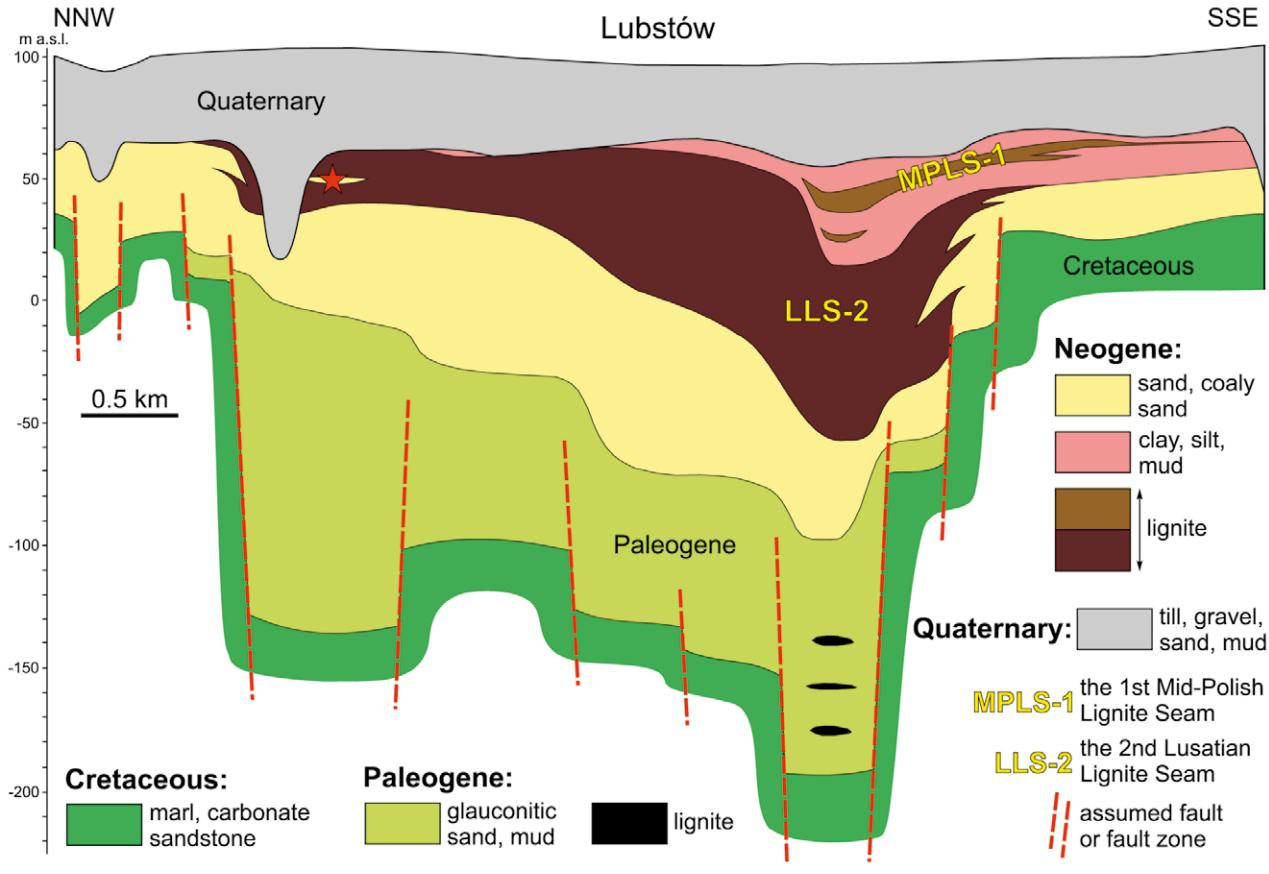


Fig. 3. Geological cross-section through the Lubstów lignite deposits (modified from Widera, 2021). Note the approximate stratigraphic position of the examined sediments within the 2nd Lusatian Lignite Seam (LLS-2).

structural features are indicated by lowercase letters. For moderate to well-sorted sediments, one or two capital letters are typically used; for instance, 'SC' for coaly sand and 'S' for sand. Poorly sorted sediments are occasionally coded using three capital letters, such as 'GSM' for sandy-muddy gravel (Tab. 2).

Moreover, the terminology for sedimentary structures is adopted from Collinson and Thompson (1982), Miall (2006, 2022), Boggs (2012), and Collinson and Mountney (2019), among others. Deformation structures – both ductile and brittle – were classified primarily according to Dżułyński and Walton (1965). In this paper, all such features (folds, faults, fractures, etc.) are denoted by the lowercase letter 'd', and are described and interpreted in detail in the main text (cf. Tabs 1, 2).

Table 2

Brief descriptions and interpretations of the facies associations, distinguished within the lignite seams (LLS-2, MPLS-1) in the Konin Basin. For facies codes see Table 1.

Facies association	Subaerial, subaqueous facies	Description	Interpretation
FA-1	subaerial: GSMm, SCm, SGMh, SCh, Sh, St, SCt	up to ~1 m thick, with an erosional base; gravel-sized sandy-muddy clasts (intraclasts, rip-up clasts) present within a sand and coaly sand matrix; facies change from massive through horizontally laminated to trough cross -stratified	sudden deposition occurred onto a flat surface in the over-bank/floodplain area from high- to low-density and turbulent flows (Farrell, 2001; Toonen *et al.,* 2016; Lepre, 2017; Rahman *et al*., 2022); unsorted sediments containing intraclasts (rip-up clasts) were derived from the natural levee
FA-2	subaqueous: Sh, SCh, SMh, Sh(d), SCh(d)	up to 0.2 m thick, with a depositional base; sub-horizontally inclined laminae; ductile deformation (load casts, flame structures) present	deposition occurred on the bottomset (i.e., the lower segment) of a crevasse-splay microdelta (lacustrine delta or prograding splay), with subaqueous deposition taking place *via* traction and suspension (Zieliński, 2014); deformation resulted from unstable density gradients or uneven sediment loading (Dżułyński and Walton, 1965; Moretti *et al.*, 1999; Burns *et al.*, 2017)
FA-3	subaqueous: Sp, Sp(d), SCp(d)	0.5–1.5 m thick, with steeply dipping laminae (up to 10–25°) and a depositional base; lateral extent >300–500 m; palaeotransport directions virtually constant over short distances; variable brecciation (brecciated to non-brecciated)	deposition occurred on the foreset (i.e., the middle segment) of a crevasse-splay microdelta, dominated by subaqueous tractional processes (Bristow *et al.*, 1999; Michaelsen *et al.*, 2000; Chomiak *et al.*, 2019)
FA-4	subaerial: St, SMt, Sh, SMCh, SCh, SCm, Sr, Sh(d), SCm(d), Sm(d)	0.1–0.4 m thick, with a depositional base; displaying horizontal lamination, massive structure, as well as ripple and trough cross-lamination; stratification is frequently disrupted by roots of peat-forming vegetation; partially brecciated	deposition occurred on the topset (i.e., the upper segment) of a crevasse-splay microdelta, with accumulation taking place above the water level of the lake (standing water); sedimentation was driven mainly by tractional processes under upper- to lower-flow regime conditions (Collinson and Thompson, 1982; Allen, 1984; Miall, 2006; Widera, 2016); subsequent brecciation was caused by hydraulic fracturing, triggered by a sudden tectonic event (Obermeier *et al.*, 2005; Owen *et al.*, 2011)
FA-5	subaerial and/ or subaqueous	quartzitic sandstones with fossilised plant roots	palaeosol horizon formed by freshwater silica dissolution and precipitation (Górniak *et al.*, 1996)
FA-6	subaerial: Sm, Sh, SCh, SCm, St, SCt, SMt, Sr, SCr	up to 0.8 m thick, with an erosional base; without the facies typical of FA-3; similar facies occur FA-4; composed of a set of alternating facies St and SMt, up to 0.6 m thick with an erosional base	deposition occurred across the entire splay surface (as flat beds) and/or as migrating ripples and small dunes, with accumulation taking place under fluctuating hydrodynamic conditions, transitioning between upper- and lower-flow regimes (Allen, 1984; Miall, 2006; Zieliński, 2014); the facies displaying alternating trough cross-stratification (facies St and SMt) are interpreted as crevasse-splay channel deposits
FA-7	subaerial: SCh(d), Sh(d), SMh(d)	up to 0.5 m thick, with deformed structure (i.e., folded and faulted) and an erosional base; clearly visible laminated clasts contain variable organic-matter content	deposition occurred on the surface of the crevasse splay as a sedimentary breccia, with clasts derived from a natural levee; folding is typical of slumping, whereas brecciation resulted from a debris flow during sediment dewatering as folding transitioned into faulting; small normal and reverse faults formed during the final stage of sedimentary breccia formation (Alsop *et al.*, 2017; Ko *et al.*, 2017; Widera, 2017)

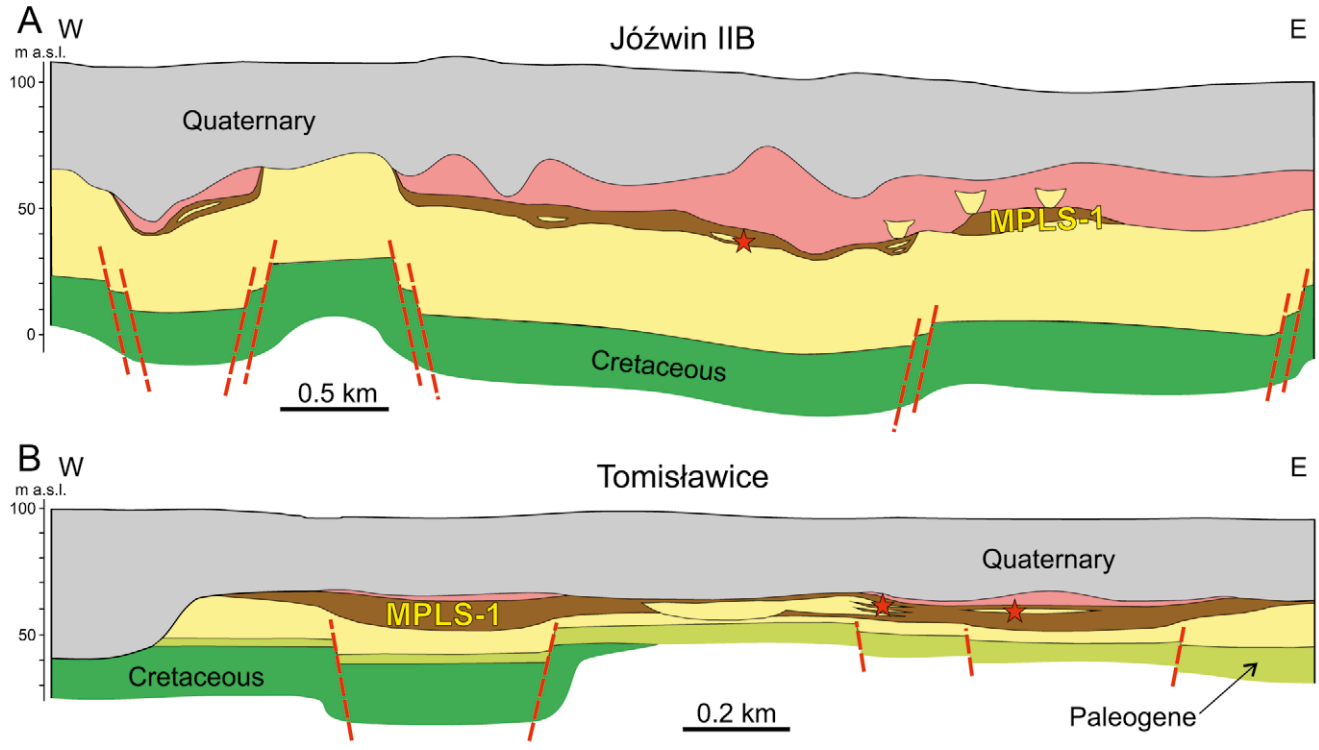


Fig. 4. Geological cross-sections through the Jóźwin IIB and Tomisławice lignite deposits (modified from Chomiak *et al.*, 2019; Widera *et al.*, 2026). Note the approximate stratigraphic position of the examined sediments within the 1st Mid-Polish Lignite Seam (MPLS-1). For explanations, see Figure 3.

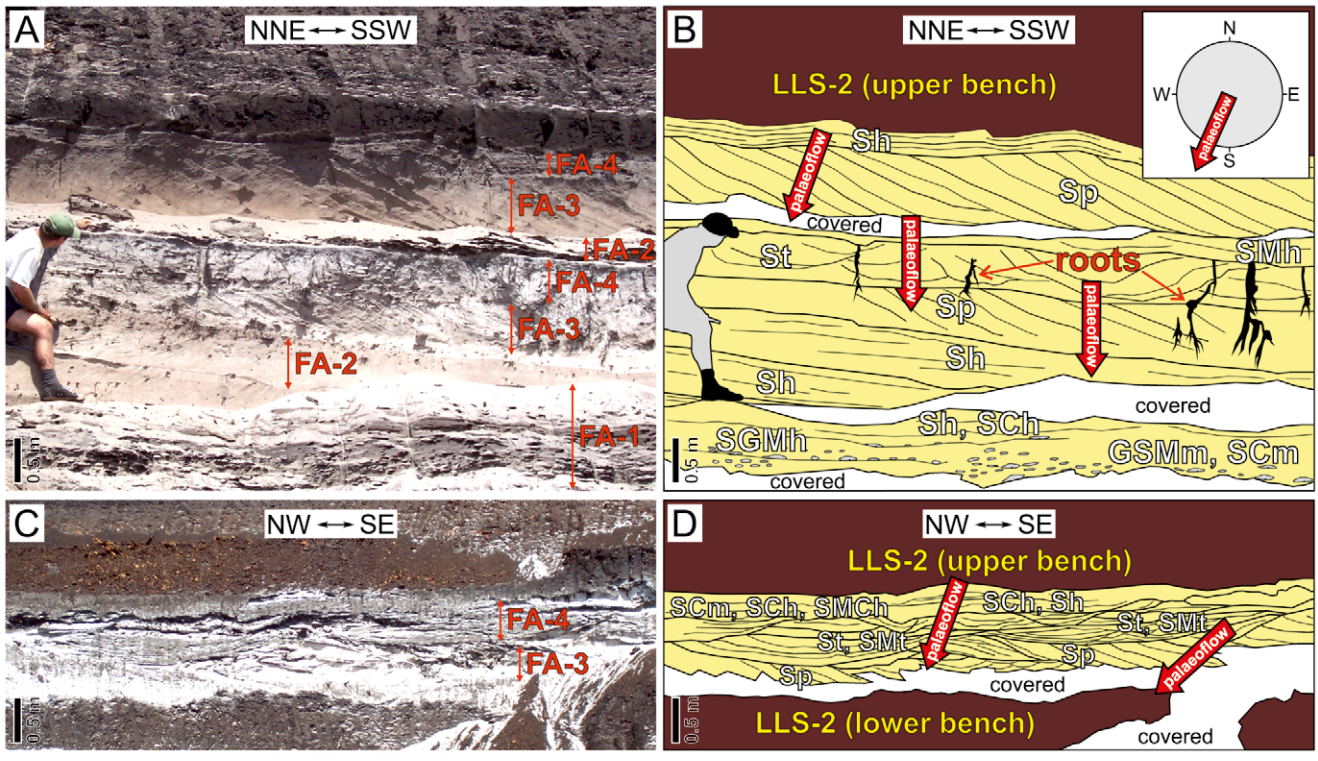


Fig. 5. Interlignite sediments in the Lubstów opencast mine. **A**, **C.** Photographic view of the outcrop sections. **B**, **D.** The corresponding line-drawings of the siliciclastic sediments, shown in Figure 5A, C, respectively. Note the key (top-right corner), explaining the averaged palaeoflow directions; for facies codes explanations, as well as descriptions and interpretations of the facies associations, see Tables 1 and 2.

RESULTS

In this study, four presently inaccessible sections were investigated in detail within the opencast lignite mines of the Konin Basin. These are, in sequence: Lubstów (north-eastern face), Jóźwin IIB (eastern face), Tomisławice South (western face), and Tomisławice North (western face; see Fig. 1). In all opencast mines, the sediments were accessible for direct observation, primarily in the exploitation face or along dewatering canals over a distance of >1 km (e.g., Jóźwin IIB opencast mine).

Lubstów section

Description: The siliciclastic sediments found within LLS-2 at Lubstów represent four facies associations: FA-1 to FA-4 (Figs 5, 6). The latter three associations recur in superposition (Fig. 5). Most of the examined sediments are clearly arranged in characteristic sequences of facies associations FA-2, FA-3, and FA-4.

FA-1 overlies the lower bench of LLS-2 with an erosional contact. At its base, it comprises massive to chaotic facies, such as sandy-muddy gravel (GSMm) and carbonaceous sand (SCm), which pass upwards into horizontally laminated facies: gravelly-muddy sand (SGMh, with aligned clasts), organic-rich, coaly sand (SCh), and sand (Sh) (Fig. 5A, B). Clasts, ranging in length from several centimetres to over 10 cm, and up to 5 cm in width, occasionally

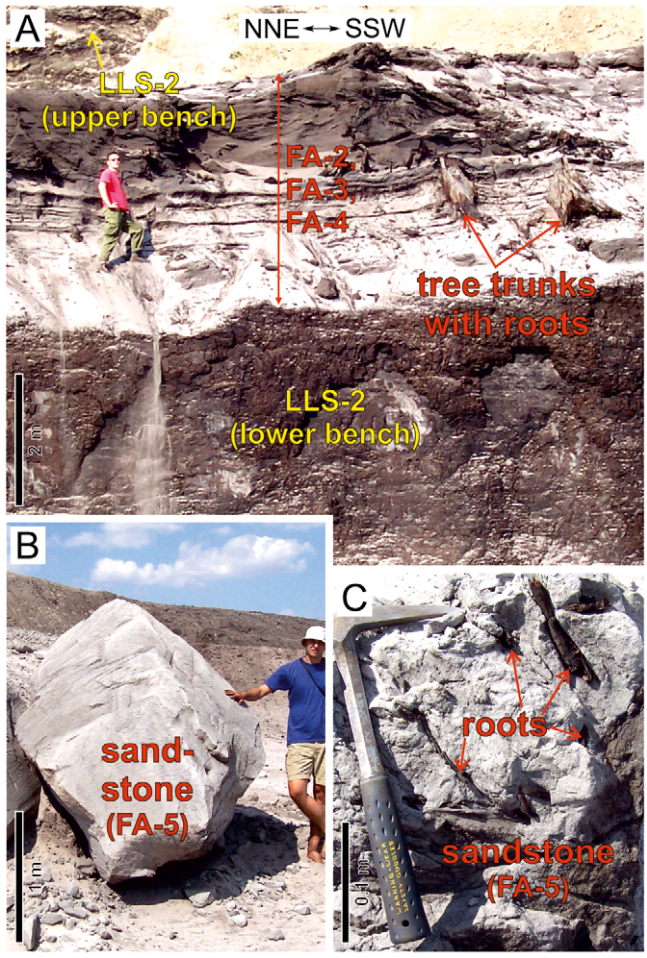


Fig. 6. Special elements and (litho)facies, associated with interlignite sediments in the Lubstów opencast mine. **A.** Tree trunks with root systems (stumps) in an upright position. **B.** Blocks of quartzite sandstones, stored in the internal dump. **C.** Details of quartzite sandstone with visible fossilised plant roots. For explanations, see the text.

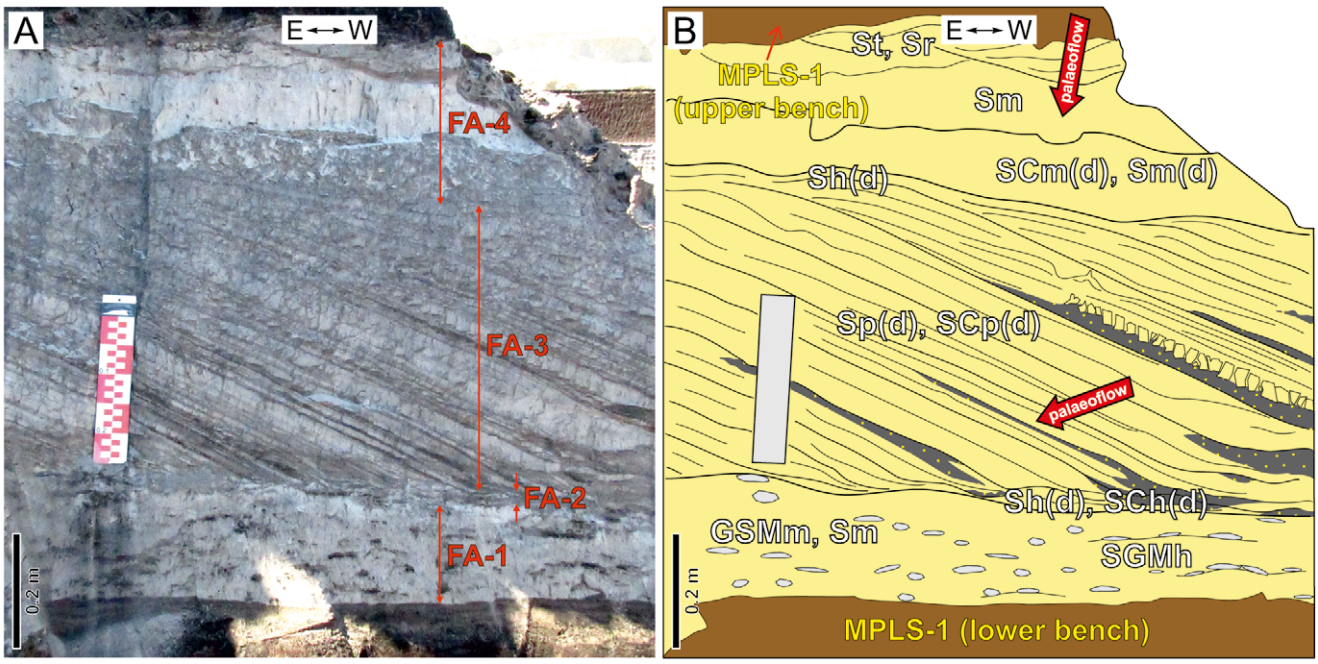


Fig. 7. Interlignite sediments in the Jóźwin IIB opencast mine. **A.** Photographic view of the outcrop section (modified from Chomiak *et al*., 2019). **B.** The corresponding line-drawing of the siliciclastic sediments, shown in Figure 7A. For facies codes explanations, as well as descriptions and interpretations of the facies associations, see Tables 1 and 2.

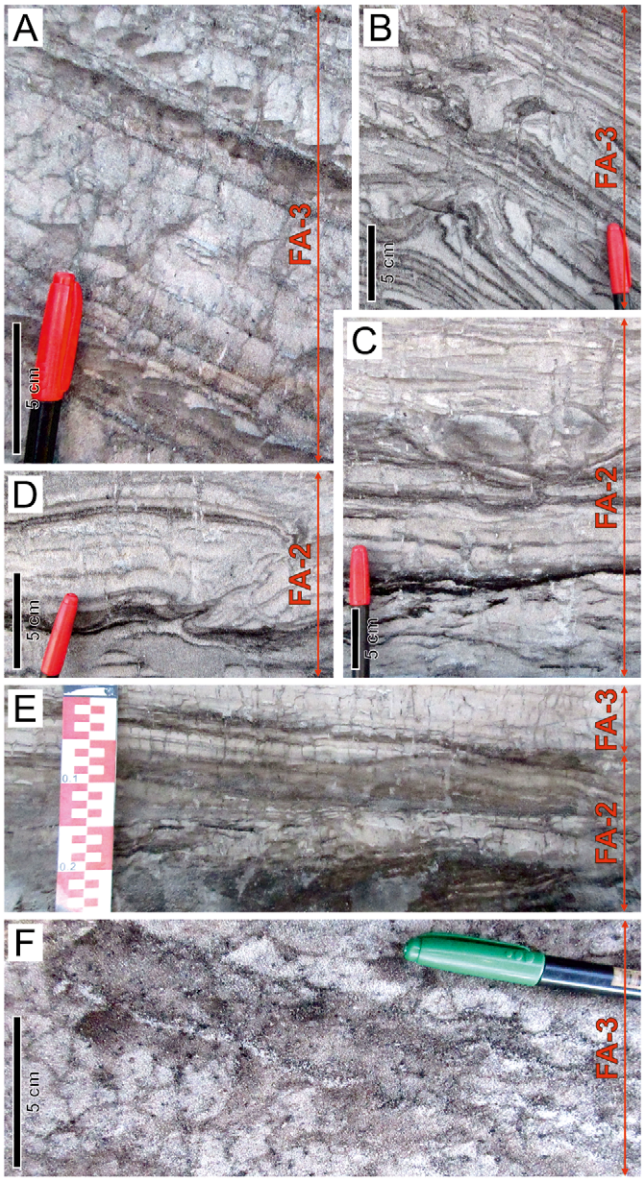


Fig. 8. Brittle and ductile deformation structures in the Jóźwin IIB opencast mine. **A**, **E**, **F.** Example of brittle deformation – tectonic breccia. **B**–**D.** Example of ductile deformations – load casts and flame structures (modified from Chomiak *et al.*, 2019). Note the superposition of brittle deformation over ductile deformation in Figure 8B–D. For explanations, see the text.

contain numerous small, fossilised roots. The total thickness of FA-1 along the lignite face ranges from 0 to ~1 m (Fig. 5A, B).

Facies association FA-1 is overlain conformably by FA-2, FA-3 and FA-4. Apart from minor lithological differences, this sequence of vertically stacked facies associations (FA-2 to FA-4) is repeated twice within the examined section. FA-2 consists of horizontally laminated sand (Sh) or muddy sand (SMh). FA-3 comprises a single facies, namely planar cross-stratified sand (Sp), whereas FA-4 includes trough cross-stratified sand (St) and muddy sand (SMt), horizontally laminated sand (Sh), coaly-muddy sand (SMCh), coaly sand (SCh), and massive coaly sand (SCm) (Table 1). All three facies associations are composed mainly of fine-grained sand, occasionally with an admixture of a finer fraction (clay and silt) or organic matter. Contacts between them (FA-2 to FA-4) are gradational (i.e., their bases are depositional; Fig. 5). Notably, facies Sp – varying in thickness from 0.2 to 1.0 m – extends over a distance of ~600 m, with laminae dipping at angles of 10–25°. Overall, the average palaeotransport direction was towards the south–southwest (Fig. 5), while the total thickness of FA-2 to FA-4 was 0.6–2.1 m.

In other parts of the Lubstów opencast mine, tree trunks with root systems (stumps) and quartzitic sandstones (FA-5) were observed (Fig. 6). Both are genetically related to the examined interlignite sands. The trunks are preserved in an upright growth position, with diameters exceeding 0.5 m (Fig. 6A). *In situ*, FA-5 has a lateral extent ranging from 5 to >100 m and a thickness of up to 2 m, whereas within the internal dump, the largest sandstone blocks of FA-5 reach volumes of 5 to >20 m^3 (Fig. 6B; Wachocki *et al.*, 2025). Furthermore, the upper, more lithified parts of these sandstones contain strongly fossilised plant roots (Fig. 6C).

Interpretation: In this study, FA-1 is interpreted as the product of rapid sedimentation from gravity-driven turbulent flows. Facies GSMm and SGMh most likely represent fossilised fragments of turf (palaeosols) preserved as clasts. Consequently, these clasts can be classified as intraclasts or rip-up clasts originating from the erosion of natural levees during flooding. They were rapidly deposited from high- to low-density flows, as indicated by the massive to poorly laminated structure of the sediment, reflecting turbulent and erosive flow dynamics (e.g., Farrell, 2001; Toonen *et al.*, 2016; Lepre, 2017; Rahman *et al.*, 2022). Towards the upper part of FA-1, intraclasts become progressively less abundant, and massive facies transition into vaguely horizontally stratified facies, such as SGMh, SCh, and Sh (Fig. 5A, B). This shift reflects a transition to lower-energy, low-density sheetflows operating over a broader depositional surface. Facies Sh and SCh formed upper-flow-regime plane beds (e.g., Allen, 1984; Miall, 2006; Zieliński, 2014).

FA-2, FA-3, and FA-4 form a distinct tripartite sequence, interpreted as components of a small lacustrine delta or crevasse-splay microdelta (e.g., Bristow *et al.*, 1999; Michaelsen *et al.*, 2000; Chomiak *et al.*, 2019). Its lower segment (FA-2), represented by facies Sh and SMh, is interpreted as a prodelta deposit that accumulated in a lake, formed on the mire surface. FA-3 represents a middle-delta foreset. This interpretation is supported by steeply dipping laminae (up to 25°), the lateral persistence of facies Sp over several hundred metres, and its gradational transition into FA-2. Furthermore, along the exposure, palaeotransport directions vary systematically (Fig. 5B, D); however, individual measurements were highly consistent over short distances, which is linked to the lobate morphology of the microdelta (Miall, 2006). FA-4 corresponds to the topset, forming the upper part of the delta. Horizontally stratified sands (Sh, SMCh, SCh) were deposited under subaerial conditions during unconfined sheetflow across the entire depositional surface (e.g., Allen, 1984; Farrell, 2001). The massive coaly sands (SCm) resulted most likely from

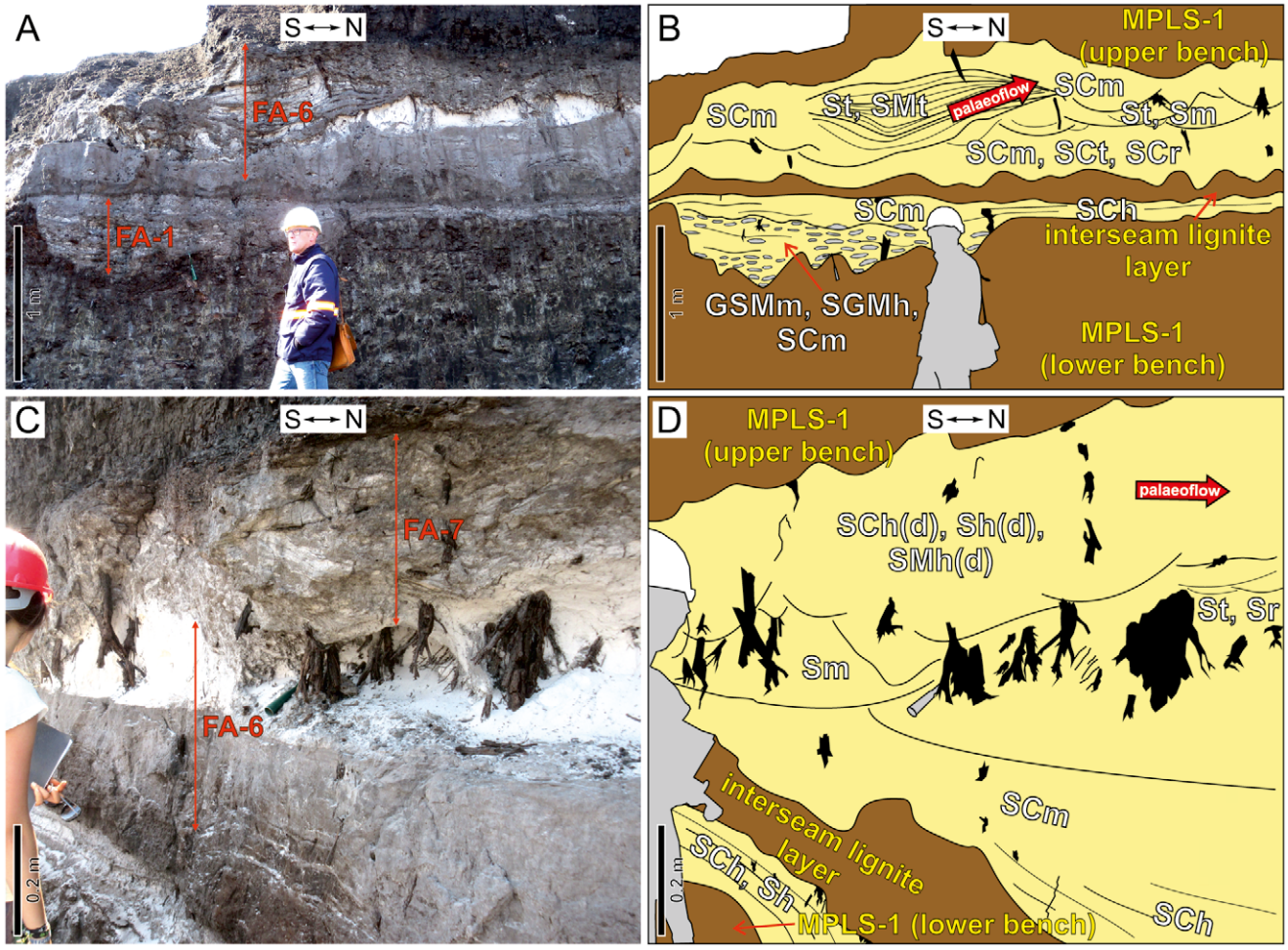


Fig. 9. Interlignite sediments in the Tomisławice opencast mine, southern site. **A**, **C.** Close-up view of the outcrop sections displaying two facies associations FA-1 and FA-6. **B**, **D.** The corresponding line-drawings of the siliciclastic sediments shown in Figure 9A, C, respectively. Note the channel-fill on the splay in Figure 9A, B and the sedimentary breccia in Figure 9C, D. For facies codes explanations, as well as descriptions and interpretations of the facies associations, see Tables 1 and 2.

subsequent soil processes or are apparently massive due to a high degree of sorting, despite being originally stratified; however, this stratification is barely discernible in the field (e.g., Chomiak *et al.*, 2019). Conversely, facies St and SMt record shallow, channelised flow and the migration of small dunes (e.g., Collinson and Thompson, 1982; Bristow *et al.*, 1999; Widera, 2016; Collinson and Mountney, 2019).

FA-5 represents unique rocks within the predominantly fine-grained Paleogene–Neogene siliciclastic sediments (and lignites) of the Polish Lowlands (Fig. 6B, C). These are freshwater quartzitic sandstones, formed within a Miocene palaeosol environment. The subcoal sands were cemented by silica derived from the dissolution of quartz grains within these deposits. This interpretation is supported by the presence of organo-quartz aggregates – confirmed *via* scanning electron microscopy (SEM) – occurring as authigenic quartz overgrowths. Consequently, the decomposition of organic matter (i.e., plant roots; Fig. 6C) and local pH fluctuations driven by organic acids induced the lithification of the unconsolidated sediment, forming FA-5 (Górniak *et al.*, 1996; Wachocki *et al.*, 2025).

Jóźwin IIB section

Description: The interlignite clastics, exposed in the Jóźwin IIB opencast mine, belong to MPLS-1. Four facies associations were distinguished in this location, namely FA-1 and FA-2 to FA-4 (Figs 7, 8). FA-1 at Jóźwin IIB is texturally and structurally similar to FA-1 identified at Lubstów (cf. Figs 5A, 5B, 7A, 7B). This association consists of facies GSMm, Sm, and SGMh. Stratification is very poorly defined, and the thickness of FA-1 varies from 20 to >40 cm where the top of the lower lignite bench has been eroded. In contrast, the remaining facies associations (FA-2 to FA-4) are exceptionally well exposed, with both sedimentary and deformational structures clearly visible (Figs 7, 8). FA-2 consists of both deformed horizontally laminated sand (Sh(d)) and coaly sand (SCh(d)). FA-3 includes deformed planar cross-stratified sand (Sp(d)) and coaly sand (SCp(d)). FA-4 encompasses deformed horizontally laminated sand (Sh(d)), massive coaly sand (SCm(d)), and massive sand (Sm(d)), as well as undeformed massive sand (Sm), trough cross-stratified sand (St), and ripple cross-laminated sand (Sr). Together, FA-2 to FA-4 form a tripartite sequence

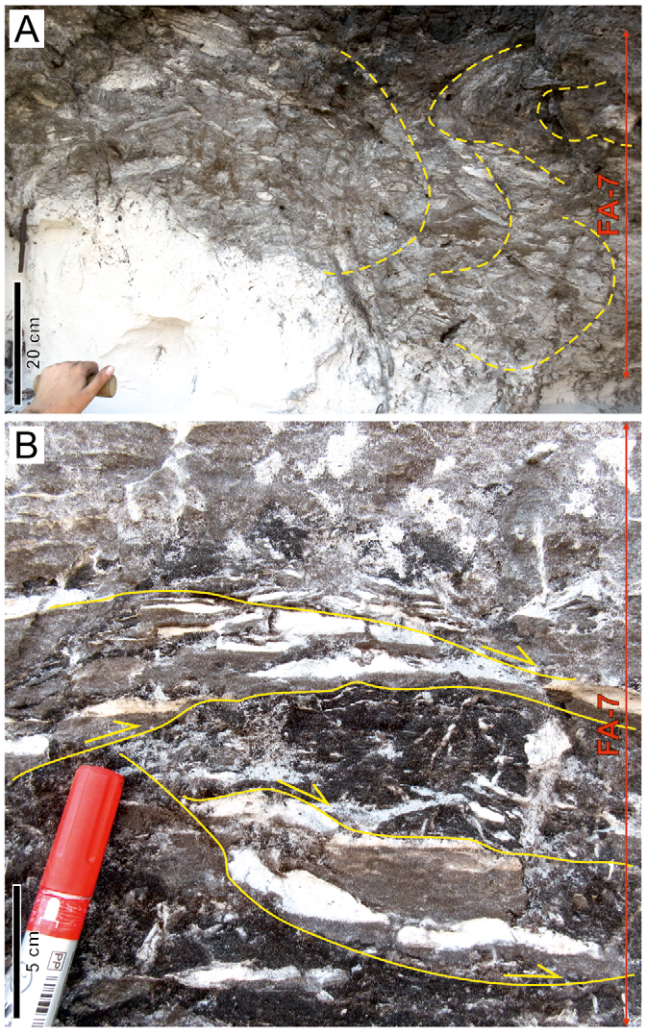


Fig. 10. Sedimentary breccia in the Tomisławice opencast mine, southern site. **A.** Example of folding (slumping). **B.** Example of faulting. For explanations, see the text.

matching that observed at Lubstów. However, these facies associations – composed predominantly of fine-grained sands – are distinguished by significant organic-matter enrichment within certain laminae and, above all, by the presence of ductile and brittle deformations. Furthermore, the transitions between FA-2, FA-3, and FA-4 are conformable, showing no evidence of erosion (Figs 7, 8; Table 1).

Interpretation: The interlignite sediments interpreted at Jóźwin IIB are typical of an initial flooding phase (FA-1), and the formation of a crevasse-splay microdelta (FA-2 to FA-4; Table 2), after a flooding river entered a shallow overbank lake. Despite their strong similarity to sediments described from the Lubstów opencast mine, sediments exposed in the Jóźwin IIB opencast mine rank among the most intensely deformed siliciclastic sediments across all Polish lignite deposits (Chomiak *et al.*, 2019).

Ductile deformation structures, such as load casts and flame structures, resulted from rheological differences between adjacent layers (Fig. 8B–D). In general, they formed due to unstable density gradients or uneven loading, which triggered sediment liquefaction (e.g., Dżułyński and Walton, 1965; Collinson and Thompson, 1982; Moretti *et al.*, 1999; Burns *et al.*, 2017; Rahman *et al.*, 2022). The breccia observed at Jóźwin IIB formed likely as a result of hydraulic fracturing, driven by high pore-water pressure. Naturally, this process requires significantly stronger seismic activity than that needed to induce ductile deformation (e.g., Obermeier *et al.*, 2005; Owen *et al.*, 2011).

The triggering mechanism of the deformation structures described within LLS-2 and MPLS-1 is likely linked to the tectonic activity of the Konin Basin, or one of its numerous grabens (Figs 3, 4; the Jóźwin IIB opencast mine covers the northernmost part of the Kleczew Graben) during the Early and Middle Miocene (Widera, 2007, 2021). Consequently, the development of these deformation structures can be attributed to seismic activity. Specifically, the ductile deformation structures were likely induced by weak seismic shocks, whereas brittle deformation – expressed through the formation of tectonic breccia – was subsequently superimposed on the ductile structures (Fig. 8). The brecciation process was probably triggered by a relatively strong tectonic shock (Chomiak *et al.*, 2019; Wachocki *et al.*, 2025).

Tomisławice South section

Description: The interlignite sediments in this section comprise three facies associations (FA-1, FA-6, and FA-7) separated by a thin lignite layer, up to 40 cm thick (Fig. 9). Notably, these predominantly fine-grained sands with erosional basal contacts – previously interpreted as crevasse-splay deposits – were the first of their kind to be identified across all lignite opencast mines in Poland (Widera, 2016).

FA-1, consisting of facies GSMm, SGMh, SCm, and SCh, corresponds almost exactly to FA-1 at Lubstów and Jóźwin IIB. In this case, however, the most prominent feature is the erosive incision into the top of the lower MPLS-1 bench, reaching a depth of up to 0.5 m (Fig. 9A, B). FA-6 erosionally overlies the aforementioned thin (up to 40 cm thick) lignite layer and starts with coaly sands (facies SCm, SCt, or SCr) and clean fine-grained sands (facies St or Sm), in which lamination is locally visible.

Consequently, facies Sm and SCm dominate in the lower part of FA-6 (Fig. 9). In its upper part, the alternating facies – namely trough cross-stratified sands (St) and muddy sands (SMt) – form a channel fill. Stratification in facies St and SMt is inclined towards the ENE (Fig. 9B). The overlying FA-7, comprising sedimentary breccia, is present only locally within the uppermost part of the interlignite succession at the Tomisławice South section. It comprises deformed (folded and faulted), horizontally laminated facies SCh(d), Sh(d), and SMh(d) (Fig. 9C, D; Table 1). Internally laminated clasts vary in colour from white through grey to black (Fig. 10). Both facies associations (FA-6 and FA-7) are penetrated by fossilised tree roots originating from the upper bench of MPLS-1 (Fig. 9).

Interpretation: FA-1 is texturally and structurally very similar across all examined sections and should therefore be interpreted in the same manner. It represents rapid deposition during the initial flooding phase (cf. the interpretation of FA-1 in Table 2). In contrast, FA-6 and FA-7

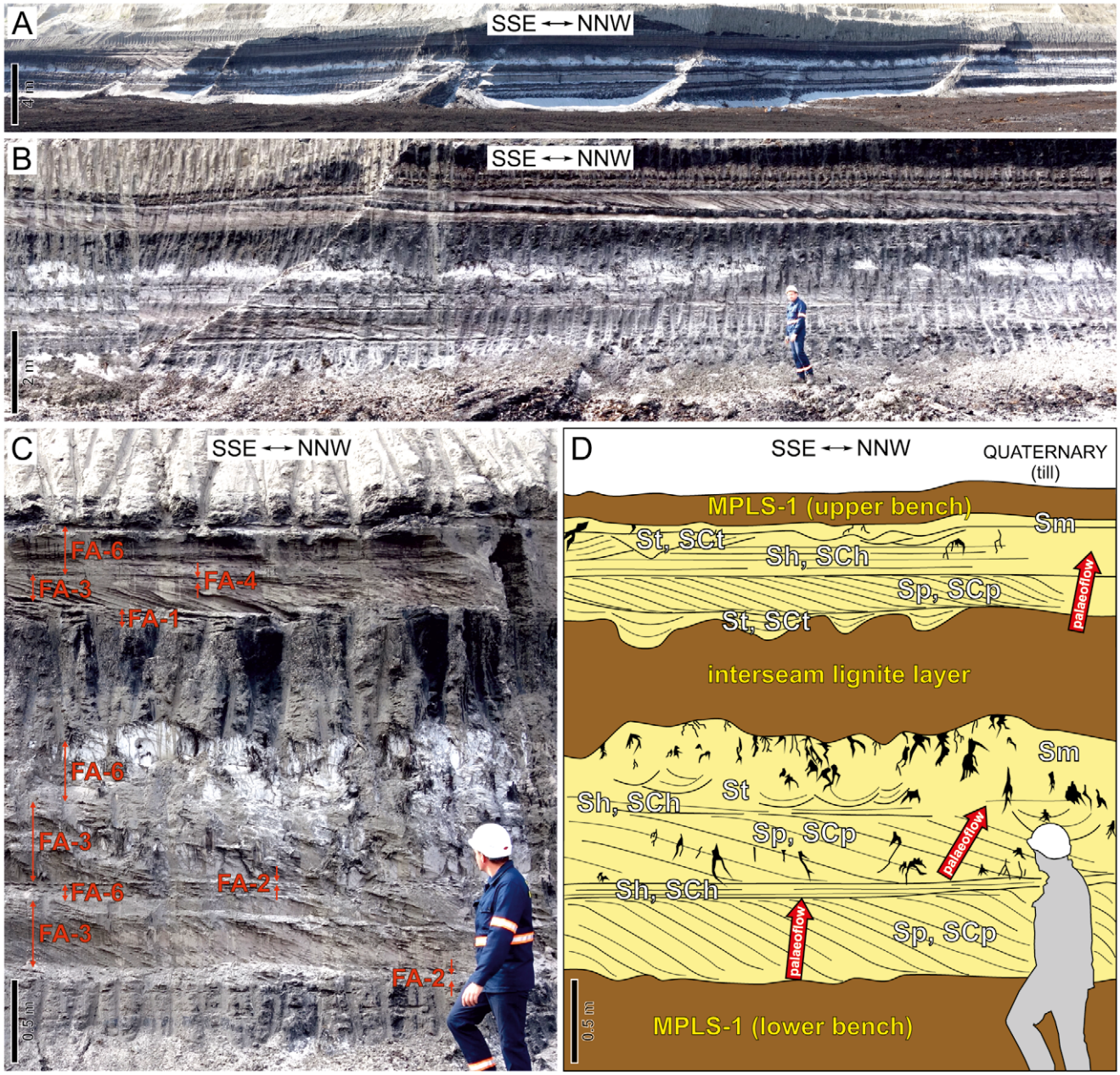


Fig. 11. Interlignite sediments in the Tomisławice opencast mine, northern site. **A**, **B.** Panoramic views of the outcrop sections. **C.** Close-up view of the outcrop section, displaying main facies associations: FA-1-FA-3, and FA-6. **D.** The corresponding line-drawing of the sediments shown in Figure 11C. Note the repeated occurrence of facies sets in the section. For facies codes explanations, as well as descriptions and interpretations of the facies associations, see Tables 1 and 2.

differ genetically from the facies associations, described in the Lubstów and Jóźwin IIB sections and warrant closer examination.

The lower part of FA-6 is interpreted as crevasse-splay sediments, formed under subaerial conditions (Lepre, 2017). Deposition initially occurred from tractional flow across the entire depositional surface (facies SCh) or *via* flow, characterised by rapid sediment dumping (facies Sm and SCm), subsequently transitioning to flow depositing on small dunes or ripples (facies St and Sr). Overall, a decrease in flow energy is observed towards the top of these sediment bodies (Collinson and Thompson, 1982; Allen, 1984; Miall, 2006; Collinson and Mountney, 2019). In contrast, the upper part of FA-6 (alternating facies St and SMt) represents a crevasse-splay channel fill (Bristow *et al.*, 1999; Burns *et al.*, 2017). Thus, the alternating occurrence of facies St and SMt reflects energy fluctuations in the flowing water (Fig. 9A, B; Miall, 1977; Allen, 1984; Bristow *et al.*, 1999; Widera, 2016).

FA-7 differs significantly from the other facies associations analysed in this study (Figs 9C, 9D, 10). It consists of sedimentary breccia (FA-7), comprising horizontally laminated heterolithics (originally natural levee sediments), such as fine-grained sands and carbonaceous muddy sands, that were subsequently deformed (facies SMh(d), SCh(d), and Sh(d)). The deformed clasts resemble those within FA-1

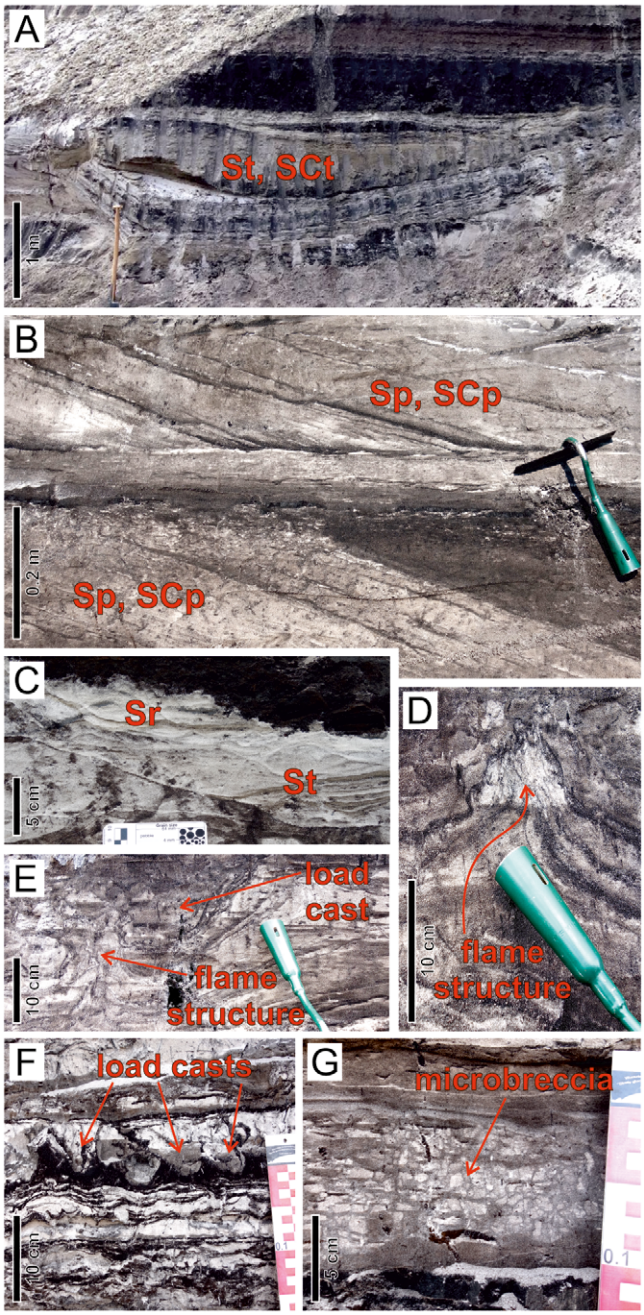


Fig. 12. Non-deformational and deformational structures in the Tomisławice opencast mine, northern site. **A**–**C.** Large- and small-scale cross-stratification. **D**–**G.** Ductile (load casts and flame structures) and brittle (tectonic microbreccia) structures. For explanations, see Table 1 and the text.

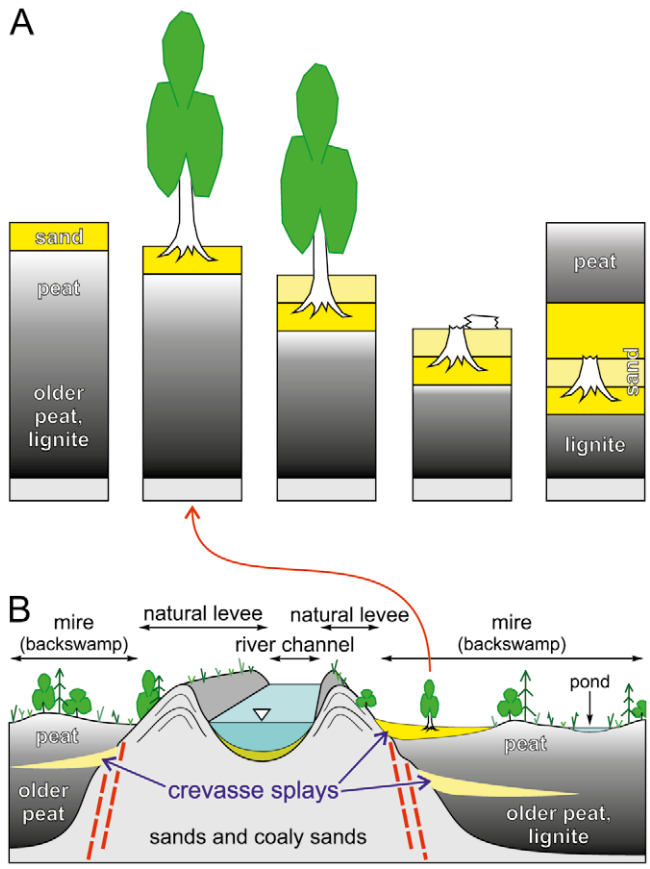


Fig. 13. Fossilisation of tree trunks in an upright position in crevasse-splay sediments (modified after Brzyski *et al.*, 1976; Gradziński and Doktor, 1995). **A.** Stages of tree trunks burial as a result of the depositional surface subsidence of the crevasse splay, caused by compaction of the underlying peat/lignite. **B.** Location of the tree growing on the top of the crevasse splay in relation to the main river channel of the adjacent mire/backswamp. For explanations, see Figure 14 and the text.

at Lubstów and Jóźwin IIB (cf. Figs 5A, 5B, 7, 9A, 9B). The presence of both folded and faulted structures within the breccia suggests that the brecciation process was triggered by a slump with ductile deformation, which rapidly transformed into a debris flow, characterised by brittle deformation. Driven by sediment dewatering, folding transitioned into faulting along small-scale synsedimentary faults, including both normal and reverse types (Fig. 10A, B). These structures provide evidence of local extensional and compressional conditions, affecting unlithified sediments during the final stages of their deposition onto the crevasse-splay surface (e.g., Alsop *et al.*, 2017; Ko *et al.*, 2017; Widera, 2017).

Tomisławice North section

Description: Three main facies associations (FA-1, FA-3, and FA-6) were distinguished within the interlignite sediments, exposed at MPLS-1 in the Tomisławice opencast mine. They are predominantly composed of fine-grained sand and varying admixtures of organic matter. FA-1 occurs only once, whereas FA-3 and FA-6 recur three times throughout the analysed section (Fig. 11). Additionally, traces of deformed FA-2 (up to 30 cm thick; cf. Fig. 12D–F) and undeformed FA-4 were observed in the Tomisławice North section (up to 10 cm thick; cf. Fig. 11C). These two associations, characterised by limited thickness (FA-2 and FA-4), are analogues to those described and interpreted in the Tomisławice and Jóźwin IIB sections.

FA-1 comprises facies St and SCt, which occur only locally within the upper part of the examined section. This association erosionally overlies a relatively thick (up to 0.8 m) lignite seam, underlies FA-3, and displays distinct trough cross-stratification (Figs 11C, 11D, 12A, 12C). In contrast, FA-3 and FA-6 predominate and can be observed along almost the entire exposure length (>300 m; Fig. 11A, B).

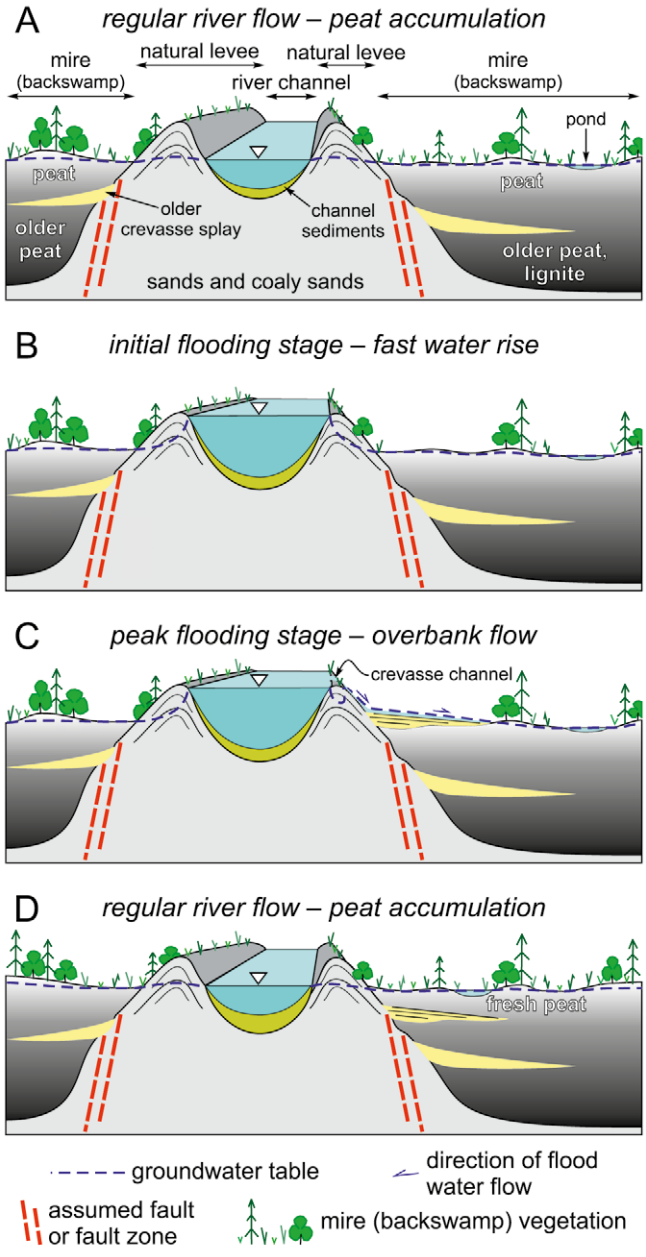


Fig. 14. Conceptual model of subaerial facies formation during a short flood. For explanations, see the text.

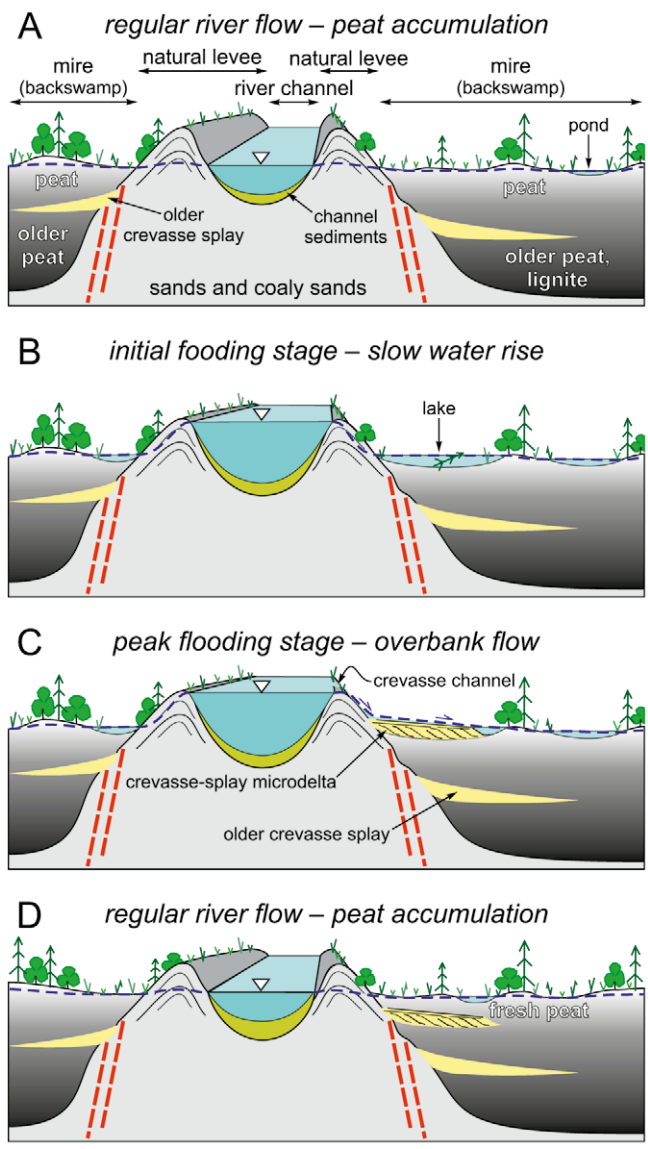


Fig. 15. Conceptual model of subaqueous facies formation during a long, regular flood. For explanations, see the text.

FA-3 includes planar cross-stratified sands (Sp) and coaly sands (SCp) with depositional basal contacts, whereas facies Sh and SCh (locally also St and SCt) belong to FA-6. The facies association FA-6 erosionally overlies FA-3. Notably, the dip direction of the laminae within facies Sp and SCp (FA-3) is remarkably consistent, ranging between NNE and NE (Fig. 11C, D).

The interlignite sediments, described from the Tomisławice North section, contain sporadic, small-scale deformation structures of various types. These include load casts, flame structures, and tectonic microbreccia (Fig. 12D–G).

Interpretation: FA-1 can be linked to the initial phases of individual flood events; thus, it consistently occurs in the lowermost part of all crevasse-splay successions. A common feature of this association is its distinctly erosional base. At the Tomisławice North section, however, FA-1 differs from the other examined sections by lacking rip-up clasts. This can be explained by its position relative to the main river channel – namely, within a more distal part of the crevasse splay. Alternatively, the interpreted FA-1 (facies St and SCt) may indicate channelised flow across the depositional surface (e.g., Collinson and Thompson, 1982; Collinson and Mountney, 2019).

FA-3 represents a well-developed middle segment of the crevasse-splay microdelta, i.e., the foreset (Fig. 11B–D). In contrast to facies Sp and SCp (FA-3), sediments typical of the bottomset and topset (facies Sh, SMh, etc.) were identified only sporadically, as they either resemble the lower layers of FA-3 or are frequently characterised by a massive structure. In the latter case, this may be attributed to good sediment sorting, laminar water flow, subsequent erosion, or the destructive role of lignite-forming vegetation (e.g., Dziamara *et al.*, 2023; Widera *et al.*, 2024; Wachocki *et al.*, 2025).

FA-6 is interpreted as the sedimentary record of relatively high-energy flows across the entire splay surface. In other words, facies Sh and SCh were deposited by sheetflows under subaerial conditions. Consequently, these horizontally laminated fine-grained sands formed under upper-flow-regime conditions. Locally present facies St and SCt, however, indicate channelised flow (e.g., Allen, 1984; Miall, 2006; Zieliński, 2014). This interpretation is supported by the fact that the contact between the deposits of FA-6 and the underlying facies associations is predominantly erosional (cf. Figs 11C, 11D, 12B).

The deformation structures described above (i.e., from the Tomisławice opencast mine) were interpreted alongside the characterisation of similar features from the Jóźwin IIB opencast mine. They are presented in this paper solely to demonstrate that such deformations occur at various scales across different lignite opencast mines within the Konin Basin (cf. Figs 8, 12D–G).

DISCUSSION

At least a few key issues that emerged during the research warrant brief discussion. The most important of these are: vertical tree trunks, subaerial *versus* subaqueous facies, and short- *versus* long-duration river floods.

Vertical tree trunks

Root traces are common in the studied interlignite siliciclastic sediments (see Figs 5, 6, 9, 11) and typically descend from the base of the overlying lignite beds/benches. Tree trunks, if preserved, occur almost exclusively within the lignite beds. The sole exception consists of coalified tree stumps (trunks with roots) found within the interlignite sands in the Lubstów opencast mine (see Fig. 6A). This represents a highly diagnostic feature that sheds light on the accumulation of these sands.

The presence of tree trunks in a vertical (upright) position within sediments or rocks is frequently described in geological literature (e.g., Brzyski *et al.*, 1976; Hámor-Vidó *et al.*, 2010; DiMichele and Falcon-Lang, 2011; Kus *et al.*, 2020). It is generally assumed that their preservation depended on rapid burial – specifically before they decomposed or fell. This process can be triggered by sudden events, such as volcanic ash fall, aeolian deposition, river floods, or rapid subsidence. Such conditions also include the formation of crevasse splays on the surface of mires (backswamps) of various ages, as has been convincingly explained, for instance, in Carboniferous coal-bearing sediments in Upper Silesia, Poland (Brzyski *et al.*, 1976; Gradziński and Doktor, 1995; see their fig. 15). As with the Carboniferous examples, the mid-Miocene crevasse splays underwent rapid aggradation. This was driven by the compaction of the underlying peat/lignite, which resulted in the creation of accommodation space (Gradziński and Doktor, 1995; Michaelsen *et al.*, 2000; Rajchl *et al.*, 2008; Mach *et al.*, 2013; Opluštil *et al.*, 2014, 2024). It is worth noting that the average peat-to-lignite compaction ratio for the entire LLS-2 is approximately 2.5 (Widera, 2015), whereas for its upper layers, this ratio can exceed 7.0 (Widera, 2019). These significant differences in compaction ratios occur because the transformation of peat into lignite is a cumulative and progressive process, driven by increasing overburden pressure, moisture loss, and the biochemical degradation of organic matter (Widera, 2015, 2024). Consequently, the degree of compaction varies vertically, depending on burial depth, the geothermal gradient, and structural loading history. This determines how accommodation space was generated over time and implies that compaction remains ongoing today at a steadily decreasing rate, although it was most intense, when the organic layers were still at the peat stage (Widera, 2019, 2021). At that time, the loading of the peat surface by an overlying sand layer caused substantial compaction, driven primarily by the expulsion of pore water.

It is evident that both the trunks and roots (stumps) are located approximately one-third of the way through the thickness of the sandy lithosome (cf. Figs 6A, 13). This indicates that these trees grew on top of the lower sand beds, rather than on the roof of the underlying lignite bench. This required a relatively long period of tree growth and a hiatus in the deposition of the interlignite sands. The duration of this hiatus in sand accumulation can be estimated as several decades, corresponding to the lifespan of the trees. This confirms that the sands in question record two to three flood events (cf. Figs 6A, 13), as documented elsewhere in the Lubstów opencast mine (see Fig. 5A, B). The best evidence for an interruption in the accumulation of interlignite sands is the presence of lignite layers occurring within them, such as those found within MPLS-1 in the Tomisławice opencast mine (cf. Figs 9, 11). The total duration of these gaps in the deposition of crevasse-splay sands (i.e., the accumulation time of intersand lignite layers) was previously estimated by the authors at approximately 50 kyr (Widera *et al.*, 2024).

Subaerial *versus* subaqueous facies

The examined interlignite siliciclastic facies, predominantly fine-grained sands, were formed during overbank flooding on the surface of a mid-Miocene mire (backswamp) and are typical of crevasse splays and crevasses with deltas (Lewin *et al.*, 2016). They can be divided into those accumulated under subaerial conditions and those formed in subaqueous environments. More specifically, certain facies developed in flowing water, whereas others were deposited in standing water within shallow lakes across the mire (Tab. 2).

The facies associations distinguished in this study can be grouped genetically and morphologically. FA-1 was identified in each examined section and was formed in a subaerial environment. It represents a sedimentary record of natural levee erosion and subsequent accumulation within the proximal part of the crevasse splay during the initial stage of flooding. FA-2 to FA-4 correspond to the three segments of a crevasse-splay delta (or microdelta), namely the bottomset, foreset, and topset. The bottomset and foreset were deposited under subaqueous conditions, whereas the topset accumulated under subaerial conditions. FA-6 also developed in a subaerial environment, typical of crevasse splays (Lewin *et al.*, 2016; Tab. 2).

In contrast, FA-5 and FA-7 can be regarded as special facies associations. FA-5 corresponds to freshwater quartzitic sandstones, associated with a palaeosol horizon, whereas FA-7 represents a sedimentary breccia. Originally, the sandstones consisted of loose sand grains deposited in subaerial and/or subaqueous crevasse splays. In the case of the sedimentary breccia, the layered sand–mud–organic sediment originated from a natural levee and was subsequently deposited on top of the subaerial crevasse splay (FA-6) *via* subaerial mass movements, specifically slumping and debris flow (Tab. 2).

Short- *versus* long-duration river floods

In studies of crevasse splays in the rock record, the rate of water-level rise in the river channel preceding a flood is seldom considered. However, the flooding rate is of fundamental importance to the formation of subaerial (flowing water) and subaqueous (standing water) facies linked to crevasse splays and crevasse-splay deltas. Therefore, these significantly different conditions of sediment accumulation in the overbank areas of mid-Miocene rivers are likely associated with variations in flood duration and intensity (Figs 14, 15).

In the case of mid-Miocene deposition linked to flooding rivers, a decisive role was played by the hydraulic conductivity (filtration coefficient) of the fine-grained sand that predominantly formed the natural levees. This coefficient ranges from 0.86 to 8.60 m/day (Pazdro and Kozerski, 1990), suggesting that flowing water required approximately from 6–58 to 12–116 days to seep through natural levees 50–100 m wide. Under such conditions, water breaching or overtopping the natural levees, eroding them, and depositing crevasse splays onto the mire surface must have been associated with a relatively rapid water-level rise in the rivers – exceeding the infiltration threshold. Moreover, most of the subaerial facies described here accumulated under precisely such conditions (Fig. 14).

Conversely, when the water-level rise in the river channels was slow (long-duration floods), the water had sufficient time to infiltrate through the natural levees. This led to a rise in the groundwater table across the mire, the expansion of ponds, and the formation of shallow lakes. These lakes, forming standing bodies of water in the proximal part of the mire (backswamp) near the river channel, received sediment accumulation during floods in the form of crevasse-splay microdeltas (Fig. 15).

CONCLUSIONS

Siliciclastic sediments, occurring in the exploited parts of the lignite seams in the Konin Basin (central Poland), provide invaluable insights into their deposition and, indirectly, into the environment, in which the peat was formed and subsequently transformed into lignite. The key findings from this study are as follows:

In the vicinity of Konin, two stratigraphically distinct mid-Miocene lignite seams (LLS-2 and MPLS-1) formed on mires (backswamps) adjacent to river channels. During floods, siliciclastic sediments – predominantly fine-grained sands, often with a coaly admixture – accumulated on their surfaces in the form of crevasse splays and crevasse-splay microdeltas.

Within these crevasse splays and microdeltas, numerous sedimentary facies can be distinguished. These formed under both subaerial and subaqueous conditions, reflecting hydrodynamic contrasts between rapidly and slowly rising river floods and their expansion across the overbank area. While crevasse splays are linked exclusively to water flowing over the inundated floodplain, the crevasse-splay microdeltas formed primarily in standing water, such as shallow lakes, located in proximal parts of the mid-Miocene mires. Although alternative explanations cannot be ruled out, the consistent relationship between facies types and environmental conditions supports the validity of the conceptual models, presented in this study.

The examined siliciclastic sediments underwent syn- and post-depositional deformation on various scales, encompassing both brittle (tectonic and sedimentary breccias) and ductile (load casts and flame structures) features. These deformation structures may indicate tectonic activity in the study area during the mid-Miocene.

The study of fine-grained sands, often with an admixture of organic matter, in the Jóźwin IIB and Tomisławice opencast mines addresses a knowledge gap, regarding the genesis of similar interlignite sediments, previously known from the Lubstów opencast mine. In effect, advances in sedimentological research over the past decade have enabled this study to clarify the origin of interlignite sediments, exposed more than two decades ago.

Acknowledgements

The authors are very grateful to both reviewers, Per Michaelsen (Ulaanbaatar, Mongolia) and Stanisław Leszczyński (Kraków, Poland), for their valuable remarks, comments and advice, which have significantly improved the quality of the current version of this paper. Furthermore, we warmly thank Michał Warchoł (Bergen, Norway) for his editorial assistance. This study was funded by statutory research funds from the Institute of Geology, Adam Mickiewicz University, allocated to M.W.

REFERENCES

Allen, J. R. L., 1984. Parallel lamination developed from upper-stage plane beds: a model based on the larger coherent structures of the turbulent boundary layer. *Sedimentary Geology*, 39: 227–242.

Alsop, G. I., Marco, S., Levi, T. & Weinberger, R., 2017. Fold and thrust systems in mass transport deposits. *Journal of Structural Geology*, 94: 98–115.

Boggs, S., 2012. *Principles of Sedimentation and Stratigraphy*. New Jersey, Prentice Hall, 218 pp.

Bristow, C. S., Skelly, R. L. & Ethridge, F. G., 1999. Crevasse splays from the rapidly aggrading, sand-bed, braided Niobrara River, Nebraska: effect of base-level rise. *Sedimentology*, 46: 1029–1047.

Bruch, A. A., Uhl, D. & Mosbrugger, V., 2007. Miocene climate in Europe-Patterns and evolution. A first synthesis of NECLIME. *Palaeogeography, Palaeoclimatology, Palaeoecology*, 253: 1–7.

Brzyski, B., Gradziński, R. & Krzanowska, R., 1976. Standing trunks of calamites in the exposure Brynów brickyard and conditions for their burial. *Rocznik Polskiego Towarzystwa Geologicznego*, 46: 159–182. [In Polish, with English summary.]

Burns, C. E., Mountney, N. P., Hodgson, D. M. & Colombera, L., 2017. Anatomy and dimensions of fluvial crevasse-splay deposits: examples from the Cretaceous Castlegate Sandstone and Neslen Formation, Utah, USA. *Sedimentary Geology*, 351: 21–35.

Chomiak, L., Maciaszek, P., Wachocki, R., Widera, M. & Zieliński, T., 2019. Seismically-induced soft-sediment deformation in crevasse-splay microdelta deposits (Middle Miocene, central Poland). *Geological Quarterly*, 63: 162–177.

Ciuk, E. & Grabowska, I., 1991. Synthetic stratigraphic section of the Tertiary in the Lubstów brown coal deposit at Lubstów, Konin District. *Biuletyn Państwowego Instytutu Geologicznego*, 365: 47–72. [In Polish, with English summary.]

Collinson, J. D. & Mountney, N. P., 2019. *Sedimentary Structures. Fourth Edition*. Dunedin Academic Press, 340 pp.

Collinson, J. D. & Thompson, D. B., 1982. *Sedimentary Structures*. Allen and Unwin, London, 207 pp.

DiMichele, W. A. & Falcon-Lang, H. J., 2011. Pennsylvanian 'fossil forests' in growth position (T0 assemblages): origin, taphonomic bias and palaeoecological insights. *Journal of the Geological Society*, 168: 585–605.

Dziamara, M., Kaczmarek, P., Klęsk, J., Wachocki, R. & Widera, M., 2023. Facies and statistical analyses of a crevasse-splay complex at the Tomisławice open-cast lignite mine in central Poland. *Geologos*, 29: 173–181.

Dżułyński, S. & Walton, E. K., 1965. *Sedimentary Features of Flysch and Greywackes*. Elsevier, Amsterdam, 274 pp.

Farrell, K. M., 2001. Geomorphology, facies architecture, and high-resolution, non-marine sequence stratigraphy in avulsion deposits, Cumberland Marshes, Saskatchewan. *Sedimentary Geology*, 139: 93–150.

Flores, R. M. & Moore, T. A., 2024. *Coal and Coalbed Gas. Future directions and opportunities (2nd ed.)*. Elsevier, Amsterdam, Netherlands–Cambridge, MA, 684 pp.

Folk, R. L., 1974. *Petrology of Sedimentary Rocks*. Hemphill Publishing Company, Austin, Texas, 182 pp.

Górniak, K., Bahranowski, K., Ratajczak, T. & Szydłak, T., 1996. Formation of quartz overgrowth in arenaceous seatearths from the Lubstów brown-coal deposit (central Poland). *Przegląd Geologiczny*, 44: 626–630. [In Polish, with English summary.]

Gradziński, R. & Doktor, M., 1995. Upright stem and their burial conditions in the coal-bearing Mudstones Series (Upper Carboniferous), Upper Silesia Coal Basin, Poland. *Studia Geologica Polonica*, 108: 129–147.

Hámor-Vidó, M., Hofmann, T. & Albert, L., 2010. In situ preservation and paleoenvironmental assessment of *Taxodiacea* fossil trees in the Bükkalja Lignite Formation, Bükkábrány open cast mine, Hungary. *International Journal of Coal Geology*, 81: 203–210.

Holdgate, G. R., Gallagher, S. J. & Wallace, M. W., 2002. Tertiary coal geology and stratigraphy of the Port Phillip Basin, Victoria. *Australian Journal of Earth Sciences*, 49: 437–453.

Kasiński, J. R. & Słodkowska, B., 2016. Factors controlling Cenozoic anthracogenesis in the Polish Lowlands. *Geological Quarterly*, 60: 959–974.

Kasztelewicz, Z., Frydrychowicz, D., Galantkiewicz, E. & Widera, M., 2025. The past, present and future of Konin Lignite Mine in central Poland. *Geologos*, 31: 45–59.

Kędzior, A., Gmur, D., Doktor, M. & Opluštil, S., 2025. Peat formation dynamics in the meandering fluvial system of the Mudstone Series (Middle Pennsylvanian), Upper Silesia Coal Basin, Poland. *Geological Quarterly*, 69: 52.

Kędzior, A., Widera, M. & Zieliński, T., 2021. Ancient and modern anastomosing rivers: insights from sedimentological and geomorphological case studies of the Triassic, Neogene and Holocene of Poland. *Geological Quarterly*, 65: 54.

Ko, K., Kim, S. W., Lee, H-J., Hwang, I. G., Kim, B. C., Kee, W-S., Kim, Y-S. & Gihm, Y. S., 2017. Soft sediment deformation structures in a lacustrine sedimentary succession induced by volcano-tectonic activities: an example from the Cretaceous Beolgeumri Formation, Wido Volcanics, Korea. *Sedimentary Geology*, 358: 197–209.

Kus, J., Dolezych, M., Schneider, W., Hofmann, T. & Visiné, R. E., 2020. Coal petrological and xylotomical characterization of Miocene lignites and in-situ fossil tree stumps and trunks from Lusatia region, Germany: Palaeoenvironment and taphonomy assessment. *International Journal of Coal Geology*, 217: 103283.

Lepre, C. J., 2017. Crevasse splay and associated depositional environments of the hominin bearing lower Okote Mbr, Koobi Fora Fm (Plio-Pleistocene) Kenya. *The Depositional Record*, 3: 161–186.

Lewin, J., Ashworth, Ph. J. & Strick, R. J. P., 2016. Spillage sedimentation on large river floodplains. *Earth Surface Processes and Landforms*, 42: 290–305.

Mach, K., Sýkorová, I., Konzalová, M. & Opluštil, S., 2013. Effect of relative lake-level changes in mire-lake system on the petrographic and floristic compositions of a coal seam, in the Most Basin (Miocene), Czech Republic. *International Journal of Coal Geology*, 105: 120–136.

Markič, M. & Sachsenhofer, R. F., 1997. Petrographic composition and depositional environments of the Pliocene Velenje lignite seam (Slovenia). *International Journal of Coal Geology*, 33: 229–254.

Markič, M. & Sachsenhofer, R. F., 2010. *The Velenje Lignite: Its Petrology and Genesis*. Geološki Zavod Slovenije, Ljubljana, 218 pp.

Miall, A. D., 1977. A review of the braided-river depositional environment. *Earth-Science Reviews*, 13: 1–62.

Miall, A. D., 2006. *The Geology of Fluvial Deposits. 4th ed*. Springer-Verlag, Berlin, Heidelberg, 582 pp.

Miall, A. D., 2022. Facies Analysis. In: Miall, A. D. (ed.), *Stratigraphy: A Modern Synthesis. Springer Textbooks in Earth Sciences, Geography and Environment*. Springer, Cham, pp. 91–174.

Michaelsen, P. & Demberelsuren, B., 2024. Petro-chemical characterization and depositional setting of a Late Permian high ash coal deposit, Central Mongolia. *Mongolian Geoscientist*, 29: 55–79.

Michaelsen, P., Henderson, R. A., Crosdale, P. J. & Mikkelsen, S. O., 2000. Facies architecture and depositional dynamics of the Upper Permian Rangal Coal Measures, Bowen Basin, Australia. *Journal of Sedimentary Research*, 70: 879–895.

Moretti, M., Alfaro, P., Caselles, O. & Canas, J. A., 1999. Modelling seismites with a digital shaking table. *Tectonophysics*, 304: 369–383.

Naworyta, W. & Urbański, P., 2025. Lignite in the Polish energy industry – a premature goodbye. *Geologos*, 31: 61–71.

Obermeier, S. F., Olson, S. M. & Green, R. A., 2005. Field occurrences of liquefaction-induced features: a primer for engineering geologic analysis of paleoseismic shaking. *Engineering Geology*, 76: 209–234.

Opluštil, S., Elbe, C., Šimůnek, Z. & Drábková, J., 2024. Paleoenvironment and vegetational history of a Middle Pennsylvanian intramontane peat swamp: an example from the Lower Radnice Coal, Kladno coalfield (Czech Republic). *International Journal of Earth Sciences*, 113: 1949–1975.

Opluštil, S., Pšenička, J., Bek, J., Wang, J., Feng, Z., Libertín, M., Šimůnek, Z., Bureš, J. & Drábková, J., 2014. T0 peat-forming plant assemblage preserved in growth position by volcanic ash-fall: A case study from the Middle Pennsylvanian of the Czech Republic. *Bulletin of Geosciences*, 89: 773–818.

Owen, G., Moretti, M. & Alfaro, P., 2011. Recognising triggers for soft-sediment deformation: Current understanding and future directions. *Sedimentary Geology*, 235: 133–140.

Pazdro, Z. & Kozerski, B., 1990. *Hydrogeologia ogólna*. Wydawnictwa Geologiczne, Warszawa, 624 pp. [In Polish.]

Piwocki, M. & Ziembińska-Tworzydło, M., 1997. Neogene of the Polish Lowlands — lithostratigraphy and pollen-spore zones. *Geological Quarterly*, 41: 21–40.

Prinz, L., Schäfer, A., McCann, T., Utescher, T., Lokay, P. & Asmus, S., 2017. Facies analysis and depositional model of the Serravallian-age Neurath Sand, Lower Rhine Basin (W Germany). *Netherlands Journal of Geosciences – Geologie en Mijnbouw*, 93: 211–231.

Rahman, M. M., Howell, J. A. & Macdonald, D. I. M., 2022. Virtual outcrop-based analysis of channel and crevasse splay sandstone body architecture in the Middle Jurassic Ravenscar Group, Yorkshire, NE England. *Journal of Geological Society*, 179: jgs2021-017.

Rajchl, M., Uličný, D. & Mach, K., 2008. Interplay between tectonics and compaction in a rift-margin, lacustrine delta system: Miocene of the Eger Graben, Czech Republic. *Sedimentology*, 55: 1419–1447.

Schäfer, A. & Utescher, T., 2014. Origin, sediment fill, and sequence stratigraphy of the Cenozoic Lower Rhine Basin (Germany) interpreted from well logs. *Zeitschrift der Deutschen Geologischen Gesellschaft*, 165: 287–314.

Słodkowska, B. & Widera, M., 2021. Vegetation response to environmental changes based on palynological research on the Middle Miocene lignite at the Jóźwin IIB open-cast mine (Konin region, central Poland). *Annales Societatis Geologorum Poloniae*, 91: 149–166.

Słodkowska, B. & Widera, M., 2022. Reconstruction of the sedimentary environment of phytogenic deposits in the Tomisławice open-cast mine (Konin Region, central Poland). *Geological Quarterly*, 66: 34.

Thomas, L., 2013. *Coal geology (2nd ed.)*. John Wiley & Sons, Ltd., Chichester, West Sussex, 444 pp.

Toonen, W. H., van Asselen, S., Stouthamer, E. & Smith, N. D., 2016. Depositional development of the Muskeg Lake crevasse splay in the Cumberland Marshes (Canada). *Earth Surface Processes and Landforms*, 41: 117–129.

Tye, R. S. & Coleman, J. M., 1989. Evolution of Atchafalaya lacustrine deltas, south-central Louisiana. *Sedimentary Geology*, 65: 95–112.

Urbański, P., Wachocki, R. & Widera, M., 2025. Sedimentary record of the late Neogene avulsion process at the Tomisławice lignite open-cast mine in central Poland – a new hypothesis. *Acta Geologica Polonica*, 75: e55.

Vessey, S. J. & Bustin, R. M., 2000. Sedimentology of the coal-bearing Mist Mountain Formation, Line Creek, Southern Canadian Cordillera: relationships to coal quality. *International Journal of Coal Geology*, 42: 129–158.

Wachocki, R., Chomiak, L., Klęsk, J., Maciaszek, P., Urbański, P., Widera, M. & Zieliński, T., 2025. Geological peculiarities from the Konin Lignite Mine, central Poland: An overview. *Geologos*, 31: 31–43.

Wachocki, R., Chomiak, L. & Widera, M., 2020. Tectonic and sedimentary deformational structures within the first Mid-Polish lignite seam – Konin Basin, central Poland. *IOP Conference Series: Earth and Environmental Sciences*, 609: 012019.

Wentworth, C. R., 1922. A scale of grade and class terms for clastic sediments. *Journal of Geology*, 30: 377–392.

Widera, M., 2015. Compaction of lignite: a review of methods and results. *Acta Geologica Polonica*, 65: 367–368.

Widera, M., 2016. Depositional environments of overbank sedimentation in the lignite-bearing Grey Clays Member: New evidence from Middle Miocene deposits of central Poland. *Sedimentary Geology*, 335: 150–165.

Widera, M., 2017. Sedimentary breccia formed atop a Miocene crevasse-splay succession in central Poland. *Sedimentary Geology*, 360: 96–104.

Widera, M., 2019. What can be learned about the deposition and compaction of peat from the Miocene lignite seam exposed in the Chłapowo Cliff on the Polish coast of the Baltic Sea? *Geology, Geophysics and Environment*, 45: 111–119.

Widera, M., 2021. *Geologia polskich złóż węgla brunatnego*. Bogucki Wydawnictwo Naukowe, Poznań, 180 pp. [In Polish.]

Widera, M., 2024. Cenozoic tectonic evolution of the main lignite-rich grabens in Poland. Part 2. Tectonics *versus* autocompaction and compaction. *Acta Geologica Polonica*, 74: e7.

Widera, M., Bechtel, A., Chomiak, L., Maciaszek, P., Słodkowska, B., Wachocki, R., Worobiec, E., Worobiec, G. & Zieliński, T., 2021a. Palaeoenvironmental reconstruction of the Konin Basin (central Poland) during lignite accumulation linked to the Mid-Miocene Climate Optimum. *Palaeogeography, Palaeoclimatology, Palaeoecology*, 568: 110307.

Widera, M., Chomiak, L. & Wachocki, R., 2023. Distinct types of crevasse splays formed in the area of Middle Miocene mires, central Poland: Insights from geological mapping and facies analysis. *Sedimentary Geology*, 443: 106300.

Widera, M., Chomiak, L., Zieliński, T., 2019. Sedimentary facies, processes and paleochannel pattern of an anastomosing river system: an example from the Upper Neogene of Central Poland. *Journal of Sedimentary Research*, 89: 487–507.

Widera, M., Dziamara, M., Klęsk, J. & Wachocki, R., 2024. Four in one: a new crevasse-splay complex in the middle Miocene

of central Poland. *Annales Societatis Geologorum Poloniae*, 94: 1–18.

Widera, M. & Klęsk, J., 2025. Poznań Clays *versus* Poznań Formation in the upper Neogene of the Polish Lowlands: Controversy about meaning, origin and age. *Geological Quarterly*, 69: 17.

Widera, M., Słodkowska, B., Worobiec, E. & Worobiec, G., 2026. Middle Miocene peat mire types from the Adamów–Konin Basin in central Poland: Lithotype and sedimentological analysis in relation to palynological data. *Acta Geologica Polonica*, 76: e83.

Widera, M., Zieliński, T., Chomiak, L., Maciaszek, P., Wachocki, R., Bechtel, A., Słodkowska, B., Worobiec, E. & Worobiec, G., 2021b. Tectonic-climatic interactions during changes of depositional environments in the Carpathian foreland: An example from the Neogene of central Poland. *Acta Geologica Polonica*, 71: 519–542.

Zachos, J., Pagani, M., Sloan, L., Thomas, E. & Billups, K., 2001. Trends, rhythms, and aberrations in global climate 65 Ma to present. *Science*, 292: 686–693.

Zieliński, T., 2014. *Sedymentologia. Osady rzek i jezior*. Wydawnictwo Naukowe UAM, Poznań, 594 pp. [In Polish.]

Zieliński, T. & Widera, M., 2020. Anastomosing-to-meandering transitional river in sedimentary record: A case study from the Neogene of central Poland. *Sedimentary Geology*, 404: 105677.